THE JOURNAL OF BIOLOGICAL CHEMISTRY VOL. 285, NO. 2, pp. 888–902, January 8, 2010

Protein Kinase Cβ Modulates Ligand-induced Cell Surface Death Receptor Accumulation

A MECHANISTIC BASIS FOR ENZASTAURIN-DEATH LIGAND SYNERGY[*][S]

Received for publication, August 20, 2009, and in revised form, November 2, 2009 Published, JBC Papers in Press, November 3, 2009, DOI 10.1074/jbc.M109.057638

Xue Wei Meng[‡§1], Michael P. Heldebrant[‡1], Karen S. Flatten[§], David A. Loegering[§], Haiming Dai[§], Paula A. Schneider[§], Timothy S. Gomez[§], Kevin L. Peterson[§], Sergey A. Trushin[¶], Allan D. Hess[**], B. Douglas Smith[**], Judith E. Karp[**], Daniel D. Billadeau[§‖], and Scott H. Kaufmann[‡§¶2]

From the Departments of [‡]Molecular Pharmacology and Experimental Therapeutics, [§]Oncology, [¶]Medicine, and [‖]Immunology, Mayo Clinic College of Medicine, Rochester, Minnesota 55905 and [**]Division of Hematologic Malignancies, Johns Hopkins Sidney Kimmel Cancer Center, Baltimore, Maryland 21231

Although treatment with the protein kinase C (PKC) activator phorbol 12-myristate 13-acetate (PMA) is known to protect a subset of cells from induction of apoptosis by death ligands such as Fas ligand and tumor necrosis factor-α-related apoptosis-inducing ligand, the mechanism of this protection is unknown. This study demonstrated that protection in short term apoptosis assays and long term proliferation assays was maximal when Jurkat or HL-60 human leukemia cells were treated with 2–5 nM PMA. Immunoblotting demonstrated that multiple PKC isoforms, including PKCα, PKCβ, PKCε, and PKCθ, translocated from the cytosol to a membrane-bound fraction at these PMA concentrations. When the ability of short hairpin RNA (shRNA) constructs that specifically down-regulated each of these isoforms was examined, PKCβ shRNA uniquely reversed PMA-induced protection against cell death. The PKCβ-selective small molecule inhibitor enzastaurin had a similar effect. Although mass spectrometry suggested that Fas is phosphorylated on a number of serines and threonines, mutation of these sites individually or collectively had no effect on Fas-mediated death signaling or PMA protection. Further experiments demonstrated that PMA diminished ligand-induced cell surface accumulation of Fas and DR5, and PKCβ shRNA or enzastaurin reversed this effect. Moreover, enzastaurin sensitized a variety of human tumor cell lines and clinical acute myelogenous leukemia isolates, which express abundant PKCβ, to tumor necrosis factor-α related apoptosis-inducing ligand-induced death in the absence of PMA. Collectively, these results identify a specific PKC isoform that modulates death receptor-mediated cytotoxicity as well as a small molecule inhibitor that mitigates the inhibitory effects of PKC activation on ligand-induced death receptor trafficking and cell death.

Death receptors play a major role in mediating the cytotoxic effects of immune effector cells (1–3). The Fas receptor, which is displayed on a variety of normal and neoplastic cells, can trigger cell death when ligated by Fas ligand (FasL)[3] on the surface of cytotoxic T cells (4). Likewise, DR4 and DR5 can trigger cell death when engaged by TRAIL, the cytotoxic ligand produced by natural killer cells and interferon-treated monocytes (5–8). Because neoplastic cells appear to be particularly sensitive to TRAIL, this agent as well as agonistic anti-DR4 and anti-DR5 antibodies are currently undergoing clinical testing as potential anticancer agents (7, 9). As a result, there is substantial interest in understanding the mechanisms of death receptor-mediated cytotoxicity and its modulation.

Signaling initiated by Fas, DR4, and DR5 has been extensively studied. According to current understanding, ligand-induced clustering of these receptors results in a conformational change in their cytoplasmic death domains, allowing binding of multimers of the adapter protein Fas-associated protein with death domain (FADD) to form the so-called DISC (10–12). This oligomerized FADD in turn binds caspase 8 and/or caspase 10 monomers (13–15), causing their juxtaposition and activation (16–18). Once activated, these initiator caspases are released to the cytosol (16), where they cleave downstream molecules to initiate the apoptotic process.

The death receptor pathway is extensively regulated at many levels. First, binding of ligand to death receptors is modulated by receptor glycosylation (19). Second, binding of ligand to potentially active receptors is altered by the presence of decoy receptors, which bind ligand but lack the required intracellular domains to initiate DISC assembly (20). Third, receptor internalization and endosomal trafficking has been observed to facilitate death signaling in some model systems (21–23). Conversely, trafficking of FADD to the nucleus has been reported to affect its availability for DISC formation (24, 25). Fourth, activation of caspase 8 is modulated by c-FLIP, an intracellular procaspase 8 homolog that can bind the DISC but lacks a catalytically competent active site (26). Some c-FLIP spice variants inhibit caspase 8 activation, whereas other splice variants facil-

* This work was supported, in whole or in part, by National Institutes of Health Grant R01 CA69008 (to S. H. K.). This work was also supported by a predoctoral fellowship (to M. P. H.) from the Mayo Foundation.

[S] The on-line version of this article (available at http://www.jbc.org) contains supplemental "Methods" and Figs. S1–S9.

[1] Both authors contributed equally to this work.

[2] To whom correspondence should be addressed: Division of Oncology Research, Gonda 19-212, Mayo Clinic, 200 First St., S.W., Rochester, MN 55905. Tel.: 507-284-8950; Fax: 507-293-0107; E-mail: Kaufmann.scott@mayo.edu.

[3] The abbreviations used are: FasL, Fas ligand; APC, allophycocyanin; DISC, death-inducing signaling complex; DR, death receptor; EGFP, enhanced green fluorescent protein; PBS, calcium- and magnesium-free Dulbecco's phosphate-buffered saline; PMA, phorbol 12-myristate 13-acetate; shRNA, short hairpin RNA; TRAIL, tumor necrosis factor-α related apoptosis-inducing ligand; PI, propidium iodide; FADD, Fas-associated protein with death domain.

itate caspase 8 activation (27–30). Fifth, it has been reported that death receptor signaling can be modulated by CARPs, E3 ubiquitin ligases that bind and presumably ubiquitylate active caspases 8 and 10 (31).

In addition, it has been suggested that PKC activation can affect sensitivity to death ligands. In particular, several groups have previously reported that treatment with PMA, a well characterized activator of PKC and several other enzymes, inhibits Fas- or TRAIL-mediated apoptosis in some cells (reviewed in Refs. 32–34). Early studies proposed several mechanisms for the ability of PMA to protect susceptible cells from death ligand-induced apoptosis, including activation of extracellular signal-regulated kinase (ERK) (35), which phosphorylates the antiapoptotic Bcl-2 family members Bcl-2 (36) and Mcl-1 (37), or activation of the transcription factor NF-κB (38), which enhances expression of a number of antiapoptotic polypeptides (39, 40). In contrast, subsequent reports provided evidence that PMA affects death signaling more directly by disrupting recruitment of FADD and procaspase 8 to the intracellular domains of ligated Fas (32, 33), DR4, and DR5 (34). These latter studies, however, left a number of questions unanswered. First, although prior results demonstrated that PMA provides short term protection from apoptosis, it has been unclear whether PMA is merely delaying the apoptotic process or affecting the number of cells that ultimately die. Second, even though a variety of PKC isoforms, including PKCα, PKCβ, PKCε, PKCθ, PKCδ, and PKCζ, have been implicated in pro- and antiapoptotic signaling (41), it remains uncertain which PKC isoforms are responsible for modulating the death receptor pathway. Third, the mechanism by which PKC activation diminishes DISC formation has remained unclear. This study was undertaken to address these issues.

EXPERIMENTAL PROCEDURES

Materials—Enzastaurin was provided by Lilly. Other reagents were purchased from the following suppliers: PMA, Hoechst 33258, camptothecin, staurosporine, dimethyl pimelimidate, and monoclonal anti-FLAG antibody (M2) from Sigma; 3-(1-(3-imidazol-1-ylpropyl)-1*H*-indol-3-yl)-4-anilino-1*H*-pyrrole-2,5-dione (catalog no. 539654) from Calbiochem; enhanced chemiluminescence reagents and Sepharose coupled to protein G from GE Healthcare; CH-11 monoclonal IgM agonistic anti-Fas from Millipore (Lake Placid, NY); *Escherichia coli* recombinant human TRAIL and agonistic anti-DR5 antibody from R & D Systems (Minneapolis, MN); FLAG-tagged recombinant FasL and FLAG-tagged recombinant human TRAIL from Alexis (San Diego); anti-phosphorylated PKC substrate antibody from Cell Signaling Technology (Beverly, MA); monoclonal antibodies to procaspase 8 and procaspase 3 as well as APC-coupled annexin V from Pharmingen; murine monoclonal antibodies to PKC-α, -β, -ε, and -θ from BD Transduction Laboratories; Alexa Fluor647-conjugated anti-mouse IgG from Invitrogen; and horseradish peroxidase-conjugated anti-mouse IgG, IgG_1, and IgG_{2b} as well as APC-conjugated goat anti-mouse IgM from Southern Biotechnology (Birmingham, AL). Monoclonal antibodies that recognize poly(ADP-ribose) polymerase, HSP90, and cleaved Bid were gifts from Guy Poirier (Laval University, Ste-Foy, Quebec, Canada), David Toft (Mayo Clinic, Rochester, MN), and Andreas Strasser (Walter and Eliza Hall Institute, Melbourne, Australia), respectively. Rabbit antiserum that recognizes a neoepitope at the C terminus of the caspase 3 large subunit (42) and mouse monoclonal anti-S peptide antibody (43) were generated as described.

Cell Culture and Transfection—HL-60 cells from Robert T. Abraham (Wyeth Pharmaceuticals, Pearl River, NY), Jurkat cells from Paul Leibson (Department of Immunology, Mayo Clinic, Rochester, MN), and the Jurkat variant I2.1 (FADD-deficient, Refs. 44, 45) were maintained in log phase in RPMI 1640 medium containing 100 units/ml penicillin G, 100 μg/ml streptomycin, 2 mM glutamine, and 10% heat-inactivated fetal bovine serum (medium A). For transfection, cells grown to a concentration of $3–4 \times 10^5$ cells/ml in medium A without antibiotics (medium B) were centrifuged at $200 \times g$ for 10 min, resuspended at 25×10^6 cells/ml in 0.4 ml of medium B, and incubated with 40 μg of the indicated plasmid DNA along with 5–10 μg of pEGFP-N1, which encodes EGFP, for 5 min. Samples were electroporated using a BTX 820 or 830 square wave electroporator (BTX, San Diego) at 280 V for 10 ms. After 5 min, cells were placed in fresh medium B and cultured for 24–48 h as indicated before treatment. Control experiments using a plasmid encoding EGFP typically indicated a 60–80% transfection efficiency as assessed by flow cytometry 24–48 h after electroporation.

Colony Forming and Cell Outgrowth Assays—To assess the effects of treatment on clonogenic survival, aliquots containing $4–8 \times 10^5$ log phase HL-60 cells in medium A were treated for 6 h with the indicated concentrations of TRAIL and/or PMA, sedimented at $100 \times g$ for 5 min, washed once with medium A, diluted into molten 0.3% (w/v) agar in the medium of Pike and Robinson (46), and plated in 35-mm gridded plates as described previously. After a 10–14-day incubation, colonies containing >50 cells were counted on an inverted microscope at ×25 magnification.

Because Jurkat cells do not form colonies under these conditions, long term survival and proliferation were assessed using a culture repopulation assay similar to that described by Simonian *et al.* (47). In brief, aliquots containing 10^6 cells in medium A were treated for 6 h with the indicated concentrations of TRAIL or CH-11 in the absence or presence of PMA, sedimented at $100 \times g$ for 5 min, washed once with medium A, and diluted into 10 ml of medium A. Flasks were examined daily to determine the point at which cell density again reached 1×10^6/ml. To provide a standard curve, aliquots containing 10, 100, 1000, 10^4, 10^5, and 10^6 untreated Jurkat cells were also diluted into 10 ml of medium A and examined for subsequent regrowth to 10^6 cells/ml.

T98G cells (American Type Culture Collection, Manassas, VA) were maintained in medium A supplemented with 1 mM pyruvate (medium C). After subconfluent monolayers were trypsinized, aliquots containing 250 cells were plated in multiple 35-mm dishes containing 2 ml of medium C and allowed to attach overnight. Graded concentrations of TRAIL and enzastaurin were then added to triplicate plates. After a 4-h incubation, plates were washed twice in serum-free RPMI 1640 medium and incubated in drug-free medium C for an additional 7 days. The resulting colonies were stained with Coomas-

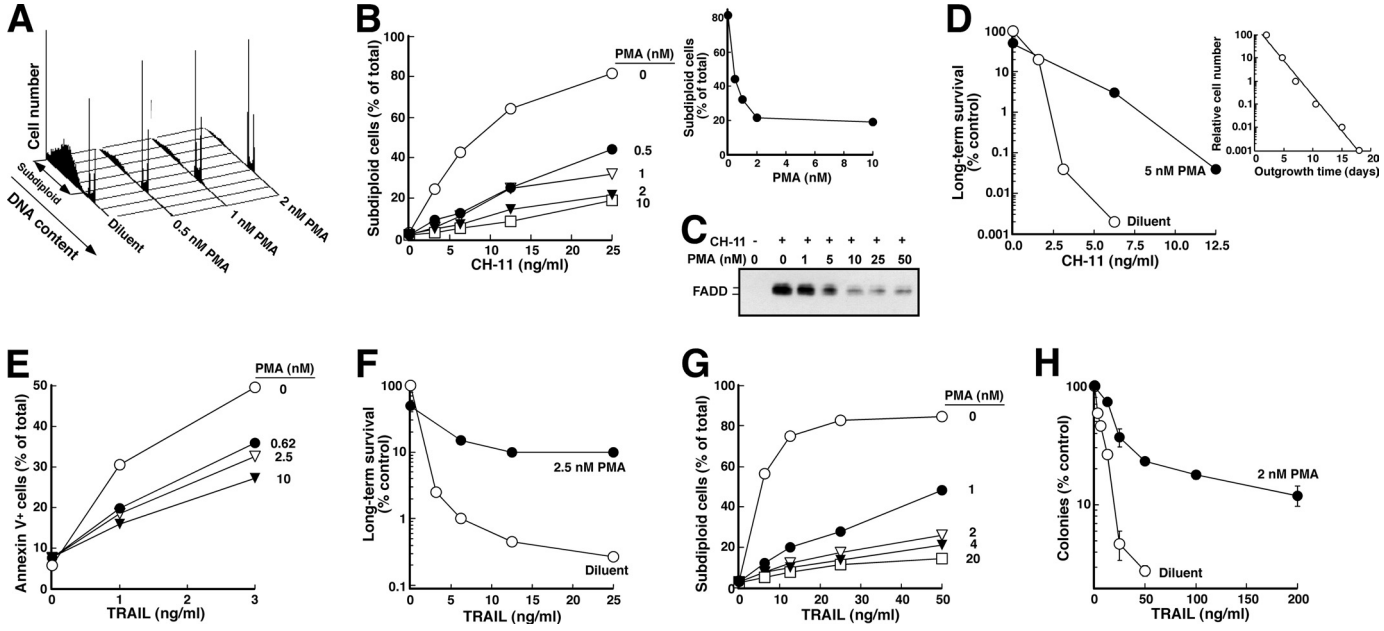

FIGURE 1. **PMA provides long term protection from agonistic anti-Fas antibody and TRAIL.** *A,* after a 5-min pretreatment with the indicated concentration of PMA or diluent (0.1% ethanol), Jurkat cells were treated for 6 h with CH-11 agonistic anti-Fas antibody at 25 ng/ml. At the completion of the incubation, samples were stained with PI and analyzed by flow microfluorimetry as described under "Experimental Procedures." *B,* results from samples in *A* and additional samples from the same experiment. *Inset,* results of treatment at 25 ng/ml CH-11 as a function of PMA concentration. *C,* after 5×10^7 Jurkat cells were treated for 90 min with 500 ng/ml CH-11 in the absence or presence of the indicated PMA concentration, cells were lysed, and the Fas DISC was immunoprecipitated as described previously (33) using anti-mouse IgM precoupled to protein G-Sepharose. Immunoprecipitates were subjected to SDS-PAGE and immunoblotting with anti-FADD antibody. *D,* after a 5-min pretreatment with 5 nM PMA or diluent, cells were treated for 6 h with the indicated concentration of CH-11. At the completion of the incubation, cells were washed in drug-free medium, diluted 1:10 in medium, and examined for ability to regrow to a density of $\sim 1 \times 10^6$ cells/ml as described previously (51). *Inset,* standard curve from this experiment, indicating time required for various dilutions of untreated cells to proliferate to a density of 1×10^6 cells/ml. *E,* after a 5-min pretreatment with the indicated concentration of PMA or diluent, Jurkat cells were treated for 6 h with the indicated concentration of recombinant human TRAIL. At the completion of the incubation, samples were stained with APC-conjugated annexin V and analyzed by flow microfluorimetry. *F,* after a 5-min pretreatment with 2.5 nM PMA or diluent, cells were treated for 6 h with the indicated concentration of TRAIL, washed in drug-free medium, diluted 1:10 in medium, and examined for ability to regrow to a density of $\sim 1 \times 10^6$ cells/ml as illustrated in *D. G,* after a 5-min pretreatment with the indicated concentration of PMA or diluent, HL-60 cells were treated for 4 h with the indicated concentration of recombinant human TRAIL, stained with PI, and analyzed by flow microfluorimetry. *H,* after a 5-min pretreatment with 2 nM PMA or diluent, cells were treated for 6 h with the indicated concentration of TRAIL, washed in drug-free medium, diluted into 0.3% agar, and assayed for ability to form colonies. *Error bars*, ±S.D. of quadruplicate aliquots.

sie Blue and counted. Diluent-treated control plates typically contained ~150 colonies. Colony forming assays using HeLa cells and HCT116 were performed similarly except that 300 (HeLa) or 500 (HCT116) cells were plated to have 150–200 colonies on the diluent-treated plates.

Apoptosis Assays —After treatment with the indicated concentrations of death ligand, PMA, and/or enzastaurin, cells were washed and stained with APC-conjugated annexin V as described (48, 49). $2–3 \times 10^4$ events were collected from the FL2 (excitation 488 nm, emission 585 ± 21 nm) and FL4 (excitation 635 nm, emission 661 ± 8 nm) channels of a BD Biosciences FACSCalibur flow cytometer and analyzed using CellQuest software (BD Biosciences). Apoptotic and nonapoptotic untransfected Jurkat cells treated with APC-annexin V alone were utilized to identify cut points for $EGFP^+$ *versus* $EGFP^-$ and annexin V^+ *versus* annexin V^- cells. Alternatively, untransfected cells were lysed at 4 °C in buffer D (0.1% (w/v) Triton X-100 and 50 μg/ml propidium iodide in 0.1% (w/v) sodium citrate) and subjected to flow cytometry to assess DNA fragmentation (45, 50). In some experiments, cells were also fixed in 3:1 (v/v) methanol/acetic acid, stained with 1 μg/ml Hoechst 33258, and examined by fluorescence microscopy for apoptotic changes in nuclear morphology (33).

Cell Fractionation—After treatment with PMA for 30–60 min, cells were harvested for fractionation. All further steps were performed at 4 °C. Cells were washed twice with PBS and then swelled for 30 min in hypotonic lysis buffer (10 mM NaCl, 3 mM $MgSO_4$, 10 mM Tris-HCl (pH 7.4 at 4 °C)) supplemented with the protease inhibitors leupeptin (10 μg/ml), pepstatin A (10 μg/ml), and α-phenylmethylsulfonyl fluoride (1 mM). Cells were lysed in a tight-fitting Dounce homogenizer until >95% of the cells were ruptured. The mitochondria and nuclei were removed by sedimentation at $4000 \times g$ for 15 min. Samples were then spun at $100{,}000 \times g$ for 1 h to separate the membrane fraction (pellet) from the cytosol (supernatant).

Plasmids—The parental pFRT-HIP and pCMS3-EGFP-HIP plasmids used for shRNA silencing were described previously (52). Isoform-specific RNA interference target sequences were selected using a custom program designed to parse the output of the GeneBee RNA secondary structure prediction program. Sequences selected for the targeted isoforms were as follows: PKCα, 5′-GAACAACAAGGAAUGACUU-3′; PKCβ, 5′-GGAAGCUGUGGCCAUCUGC-3′; PKCε, 5′-GCCACCCUUCAAACCACGCAUU-3′; and PKCθ, 5′-UUGGAUGAGGUGGAUAAA-3′.

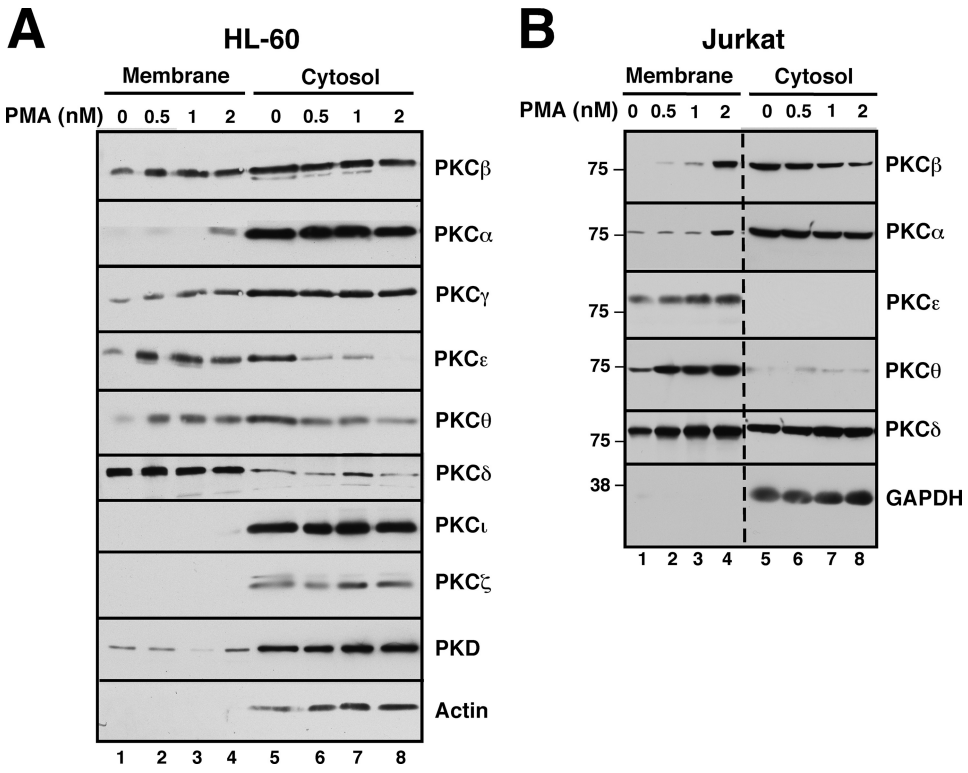

FIGURE 2. **PMA-induced translocation of PKC isoforms.** HL-60 (*A*) or Jurkat cells (*B*) were treated for 1 h with the indicated concentration of PMA. After washing, mechanical disruption, and removal of nuclei by sedimentation at 800 × *g*, the postnuclear supernatant was fractionated into cytosol (280,000 × *g* supernatant) and membranes (280,000 × *g* pellet). Aliquots containing 50 μg of protein were subjected to SDS-PAGE, transferred to nitrocellulose, and probed with antibodies to the indicated antigen. *Dashed line* in *B* indicates juxtaposition of nonadjacent wells from the same piece of x-ray film.

To generate Fas fused at its C terminus with S peptide (Fas-S peptide), cDNA encoding full-length Fas (GenBank™ accession number M67454) was isolated by reverse transcription-PCR using a 3′ primer designed to add a linker and S peptide (GAGAGAGAGGAP)MKETAAAKFERQHMDS in-frame at the C terminus. The PCR product was cloned into pcDNA3.1 using EcoRI and XbaI.

Cell Lysis—After treatment with PMA and/or death ligands as indicated in the figures, cells were washed once with ice-cold PBS and resuspended at a concentration of 30×10^6 cells/ml in DISC buffer (1% (w/v) Triton X-100, 1% (v/v) glycerol, 150 mM NaCl, 50 mM Tris-HCl (pH 7.5 at 4 °C)) supplemented with the protease inhibitors leupeptin (10 μg/ml), pepstatin A (10 μg/ml), and α-phenylmethylsulfonyl fluoride (1 mM) and the phosphatase inhibitors NaF (100 mM), NaP_2O_7 (100 mM), and Na_3VO_4 (1 mM). After a 30-min incubation at 4 °C, lysates were clarified by centrifugation at 18,000 × *g* for 15 min and transferred to fresh tubes.

Assay for Ligand Binding—To measure the binding of death ligands, 1×10^6 cells were incubated with agonistic CH-11 anti-Fas antibody or 1 μg/ml anti-FLAG antibody plus FLAG-tagged FasL or FLAG-tagged TRAIL in the absence or presence of PMA for 90 min at 37 °C. Cells were then quickly cooled, washed twice with ice-cold PBS containing 2% (v/v) heat-inactivated fetal bovine serum, and incubated with APC-conjugated anti-mouse IgM (for CH-11 binding) or Alexa Fluor647-labeled anti-mouse IgG (to detect ligand-bound anti-FLAG) for an additional 45 min on ice. Following two washes with ice-cold PBS, cells were resuspended in 4% formaldehyde in PBS and stored in the dark at 4 °C for <18 h until flow microfluorimetry was performed.

Biotinylation of Cell Surface Proteins and Fas Internalization Assay—For cell surface biotinylation as well as phosphorylation analysis, we created JFSD9 cells, which stably express Fas-S peptide, by transfecting the Fas-deficient line JM14A5 (45, 53) with pcDNA3.1 encoding Fas-S peptide. After selection in medium A containing 400 μg/ml G418 and cloning by limiting dilution, this line was chosen from among other clones because Fas was readily detectable on its surface by flow cytometry. Following treatment as specified in the figure legends, aliquots were quickly chilled by adding 4 volumes of ice-cold PBS containing 0.1 mM $CaCl_2$ and 1 mM $MgCl_2$ (PBS-CM) and washed three times with the same buffer. Cell surface proteins were biotinylated by incubating cells in 1.0 ml of PBS-CM containing 1 mM NHS-LC-Biotin (Pierce) on ice for 1 h. The reaction was stopped by incubating cells with ice-cold PBS-CM containing 100 mM glycine. After three washes with PBS-CM, cells were lysed in 1.0 ml DISC buffer as described above. Following clarification of the lysates, Fas was pulled down by incubating lysates for 2–3 h at 4 °C with anti-S peptide antibody covalently coupled to agarose and then washing the bound proteins as described (49). After release from beads and SDS-PAGE as described below, polypeptides were transferred to nitrocellulose and visualized using horseradish peroxidase-coupled streptavidin or anti-S peptide antibody.

DISC Immunoprecipitation—To isolate the Fas DISC, aliquots containing 5×10^7 cells were resuspended in 10 ml of medium A and incubated with diluent or 10 μM enzastaurin for 30 min. Following addition of PMA and/or CH-11 (final concentrations 20 nM and 500 ng/ml, respectively), the incubation was continued for an additional 90 min at 37 °C. Cells were then sedimented at 200 × *g* for 10 min and lysed in 1 ml of DISC buffer on ice for 30 min. After the lysate was cleared by centrifugation at 18,000 × *g* for 15 min, an aliquot of supernatant (4 mg of protein) was transferred to a new tube containing 30 μl of beads with rabbit anti-mouse IgM antibody cross-linked to protein G-Sepharose. Beads were rotated at 4 °C for 90 min and washed five times in DISC buffer. Bound polypeptides were released by boiling the beads for 5 min with 40 μl of SDS sample buffer and loaded on SDS-polyacrylamide gels.

Sample Preparation and SDS-PAGE—After drug treatment or fluorescence-activated cell sorting, cells were sedimented at

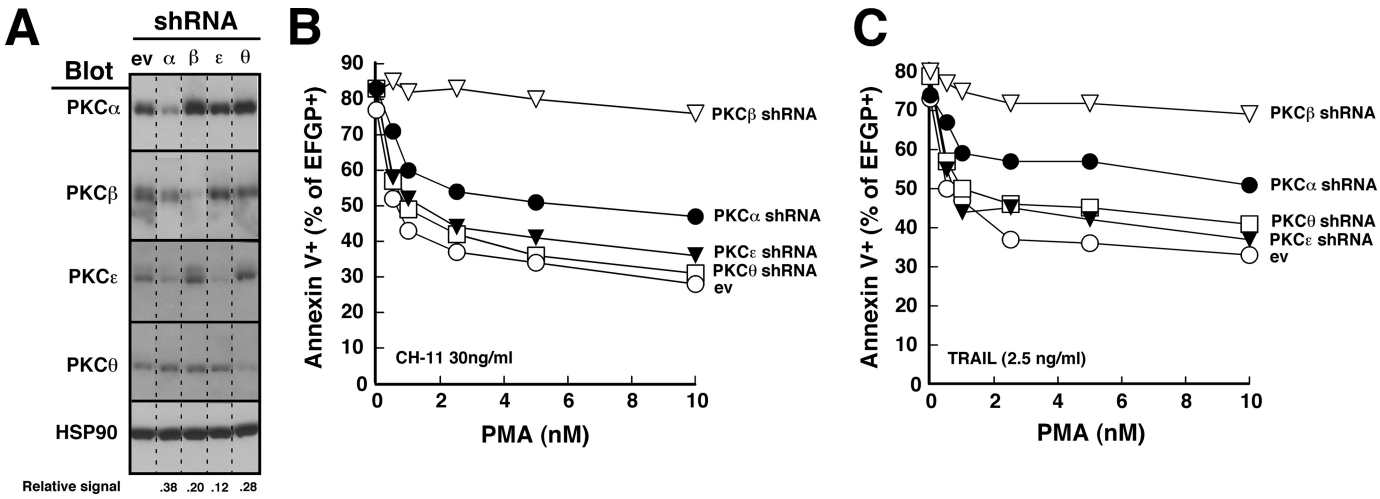

FIGURE 3. **PKCβ shRNA selectively diminishes the protective effect of PMA.** *A,* 48 h after transfection with empty vector (*ev*) or shRNA targeting the indicated PKC isoform, cell lysates from unsorted Jurkat cells were subjected to SDS-PAGE followed by immunoblotting for the indicated PKC isoform. HSP90 served as a loading control. *Dashed lines* between lanes indicate that intervening lanes from additional time points have been removed to simplify this figure. *Numbers below lanes*, relative signal intensity of targeted PKC isoform compared with empty vector after correction for Hsp90 loading. *B* and *C,* 48 h after transfection of Jurkat cells with 40 μg of empty vector or shRNA targeting the indicated PKC isoform (along with 5 μg of plasmid encoding EGFP), cells purified on Ficoll-Paque step gradients were treated for 5 h with the indicated concentration of PMA along with 30 ng/ml CH-11 (*B*) or 2.5 ng/ml TRAIL (*C*). At the completion of the incubation, cells were stained with APC-conjugated annexin V and analyzed by two-color flow cytometry (49) as illustrated in supplemental Fig. S2. The percentage of $EGFP^+$ (shRNA-transfected) cells that bound annexin V is indicated. In the absence of CH-11 or TRAIL, fewer than 20% of the cells were apoptotic.

200 × *g* for 10 min, washed once with ice-cold RPMI 1640 medium containing 10 mM HEPES (pH 7.4 at 4 °C), solubilized in buffered 6 M guanidine hydrochloride under reducing conditions, and prepared for electrophoresis (54). Aliquots containing 50 μg of protein (estimated by the bicinchoninic acid method as described in Ref. 55) were separated on SDS-polyacrylamide gels, electrophoretically transferred to nitrocellulose, and probed as described (56, 57). Where indicated, signals on x-ray film were quantitated using ImageJ software.

Apoptosis Assays in Primary Leukemia Isolates—After informed consent was obtained, samples of bone marrow were harvested from acute myelogenous leukemia patients prior to chemotherapy according to an IRB-approved protocol. Following sedimentation on a Ficoll-Paque (1.077 g/cm^3) step gradient (58), the mononuclear cells were recovered and counted on a hemocytometer. Aliquots containing 1×10^6 cells in 1 ml of medium A were incubated for 24 h in the presence of varying concentrations of enzastaurin and/or TRAIL, sedimented, lysed in buffer D, and analyzed for DNA content by flow microfluorimetry as described above. A minimum of 20,000 events/sample was counted.

Statistics—Unless otherwise indicated, experiments were repeated at least three times with similar results. Where results of multiple experiments are summarized, data are expressed as the mean ± S.D. of the indicated number of independent experiments. Groups were compared using two-sided Student's *t* tests (unpaired unless indicated).

RESULTS

Low Nanomolar PMA Concentrations Provide Short and Long Term Protection from Death Ligand-induced Toxicity—To extend our earlier observation that PMA inhibits death ligand-induced apoptosis, we examined the effects of various PMA concentrations on death induced by the agonistic anti-Fas antibody CH-11. These studies demonstrated that PMA inhibited CH-11-induced apoptosis in Jurkat cells (Fig. 1, *A* and *B*) with half-maximal inhibition at 0.5 nM (Fig. 1*B, inset*). This protection occurred over the same range of PMA concentrations that inhibited DISC formation (Fig. 1*C*), consistent with the hypothesis (32–34) that diminished DISC formation plays a role in the PMA-induced protection from death ligand-induced death.

To rule out the possibility the PMA inhibits the development of apoptotic stigmata without affecting the number of cells that ultimately die (59), we examined long term survival of CH-11-treated Jurkat cells using a culture repopulation assay. As indicated in Fig. 1*D*, PMA markedly enhanced the ability of Jurkat cells to grow back after Fas receptor ligation. PMA similarly inhibited TRAIL-induced apoptosis (Fig. 1*E*) and enhanced long term survival in these cells (Fig. 1*F*). Thus, low nanomolar PMA concentrations affect the number of cells killed by death ligands rather than merely affecting the kinetics of apoptosis.

Although the majority of previous studies examining the effect of PMA on death ligand-induced apoptosis were performed in Jurkat cells, the protective effect of PMA was not limited to this cell line. PMA also protected HL-60 cells (Fig. 1*G*)[4] and T98G glioblastoma cells (supplemental Fig. S1) from TRAIL-induced apoptosis. Clonogenic assays confirmed that PMA likewise enhanced the ability of cells to survive and multiply after TRAIL treatment (Fig. 1*H*). Thus, PMA provided long lasting protection against death ligand-induced cytotoxicity in multiple cell types.

Dose-dependent Activation of Specific PKC Isoforms—In an initial attempt to identify PKC isoform(s) that might contribute to PMA-induced protection from death ligand-induced apo-

[4] Because HL-60 cells lack the Fas receptor (94), the effects of Fas ligation were not studied in this cell line.

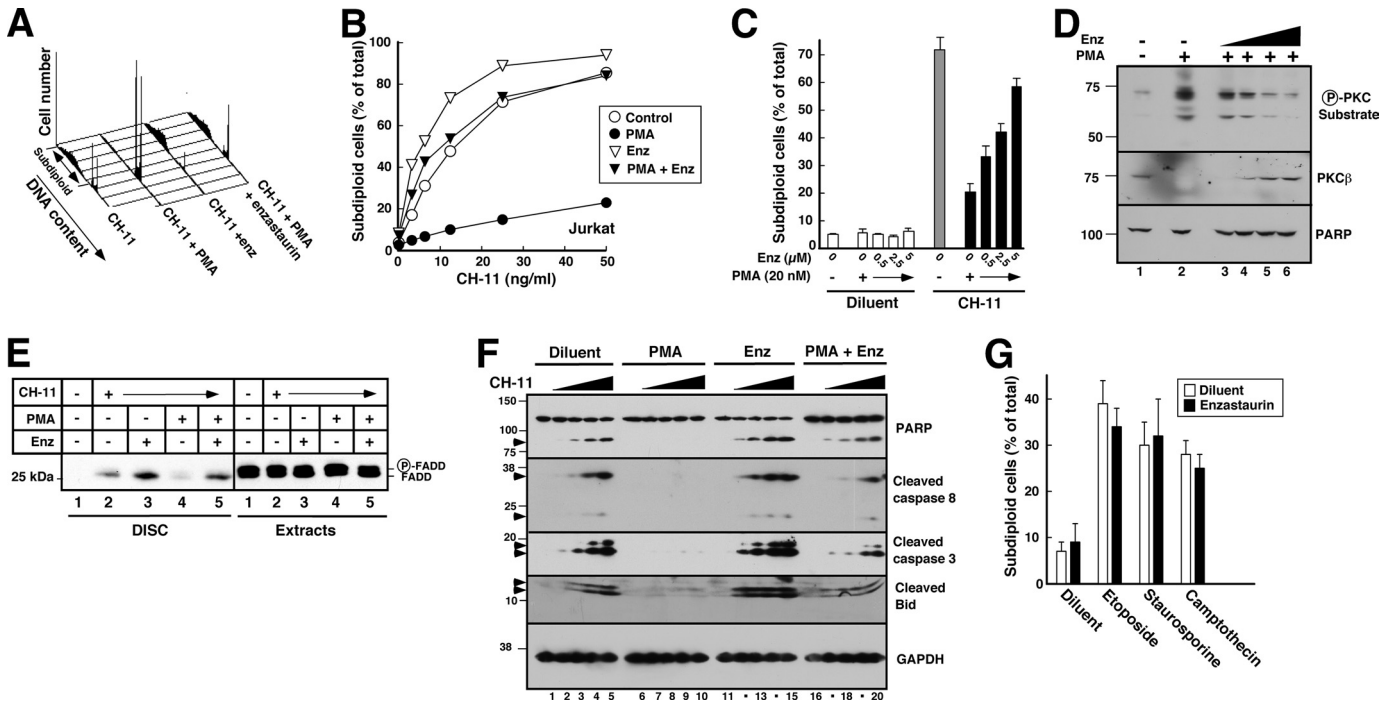

FIGURE 4. **Enzastaurin inhibits the effect of PMA on CH-11-induced apoptosis.** *A,* after a 5-min pretreatment with 20 nM PMA or diluent (0.04% ethanol) and 10 μM enzastaurin or diluent (0.02% DMSO), Jurkat cells were treated for 6 h with 25 ng/ml CH-11 agonistic anti-Fas antibody, stained with PI, and analyzed by flow microfluorimetry. *B,* results from samples in *A* and additional samples from the same experiment. *C,* after a 5-min pretreatment with 20 nM PMA or diluent and the indicated concentration of enzastaurin or diluent, Jurkat cells were treated for 6 h with CH-11 agonistic anti-Fas antibody at 50 ng/ml, stained with PI, and analyzed by flow microfluorimetry. *Error bars,* ± S.D. of three independent experiments. *D,* after log phase Jurkat cells were treated for 1 h with diluent (*lanes 1* and *2*) or enzastaurin (*Enz*) at 1.25, 2.5, 5, or 10 μM (*lanes 3–6,* respectively) without (*lane 1*) or with 20 nM PMA (*lanes 2–6*), whole cell lysates were prepared and subjected to immunoblotting with antibodies that recognize phosphorylated PKC substrates (*top*), PKCβ (*middle*) or, as a loading control, poly(ADP-ribose) polymerase (*PARP*) (*bottom*). *E,* following preincubation with 10 μM enzastaurin or diluent for 30 min, Jurkat cells (5×10^7) were treated for 90 min with 500 ng/ml CH-11 in the absence or presence of 20 nM PMA as indicated. The Fas DISC was isolated from cell extracts (4 mg of protein) using anti-mouse IgM precoupled to protein G-Sepharose. Immunoprecipitates and aliquots containing 50 μg of cell extract protein were subjected to SDS-PAGE, transferred to nitrocellulose, and probed with anti-FADD antibody. *F,* after a 5-min pretreatment with 20 nM PMA or diluent and 10 μM enzastaurin or diluent, Jurkat cells were treated for 6 h with diluent (*lanes 1, 6, 11,* and *16*) or CH-11 at 3.125 (*lanes 2, 7, 12,* and *17*), 6.25 (*lanes 3, 8, 13,* and *18*), 12.5 (*lanes 4, 9, 14,* and *19*), or 25 ng/ml (*lanes 5, 10, 15,* and *20*). At the completion of the incubation, whole cell lysates prepared from washed cells were subjected to SDS-PAGE, transferred to nitrocellulose, and probed with antibodies to the indicated antigen. *GADPH,* glyceraldehyde-3-phosphate dehydrogenase. *G,* after a 30-min pretreatment with 10 μM enzastaurin or diluent, Jurkat cells were treated for 6 h with 25 μM etoposide, 1 μM camptothecin, or 25 nM staurosporine and then assayed for DNA fragmentation. *Error bars,* ± S.D. of three independent experiments.

ptosis, cells were treated with various PMA concentrations and then fractionated into cytosol and membranes to separate inactive from active species (60–62). Immunoblotting demonstrated that PMA causes translocation of several PKC isoforms over the range of concentrations that protect Jurkat and HL-60 cells (Fig. 2). In particular, PMA caused a dose-dependent translocation of PKCα, PKCβ, PKCε, and PKCθ from cytosol to membranes in both cell lines. In contrast, other isoforms such as PKCγ, PKCδ, PKCι, PKCζ, and PKCη and the closely related enzyme PKD did not translocate or translocated in only one of the lines (Fig. 2*A* and data not shown). These observations raised the possibility that PKCα, PKCβ, PKCε, and/or PKCθ might be responsible for the effects of PMA on death ligand-induced killing.

Predominant Role for PKCβ in the Protective Effects of PMA—To further assess the role(s) of these various isoforms in protecting cells from death ligand-induced apoptosis, we created isoform-selective RNA interference constructs for PKCα, PKCβ, PKCε, and PKCθ. When Jurkat cells were transiently transfected with the indicated constructs and harvested for immunoblotting, there was extensive reduction of target protein levels with minimal alteration of levels of the nontargeted PKC isoforms (Fig. 3*A*). In further experiments, this down-regulation was maximal at 48 h and was sustained for 24–48 h thereafter.

In subsequent studies, cells were co-transfected with these RNA interference constructs and, to mark transfected cells, plasmid encoding EGFP. After cells were incubated for 2 days to allow target protein down-regulation, diluent or varying concentrations of PMA were added 5–10 min before the death ligand. As was the case with untransfected cells (Fig. 1), treatment with PMA protected empty vector-transfected cells from death ligand-induced apoptosis (Fig. 3, *B* and *C*, and supplemental Fig. S2). The percentage of cells undergoing CH-11-induced apoptosis was diminished from ~80% in the absence of PMA to ~30% in the presence of 10 nM PMA (Fig. 3*B*). Similar results were observed with TRAIL treatment (Fig. 3*C*). Thus, transfection *per se* did not alter the behavior of the cells. This ability of PMA to protect from death ligand-induced apoptosis was also not substantially altered by transfection with shRNA directed against PKCε or PKCθ (Fig. 3, *B* and *C,* and supplemental Fig. S2).

PKCα shRNA induced limited protection from PMA. When cells were treated with 30 ng/ml CH-11 in the presence of 5 nM PMA, for example, the percentage of apoptotic cells increased from 33% in cells transfected with empty vector to 50% in cells

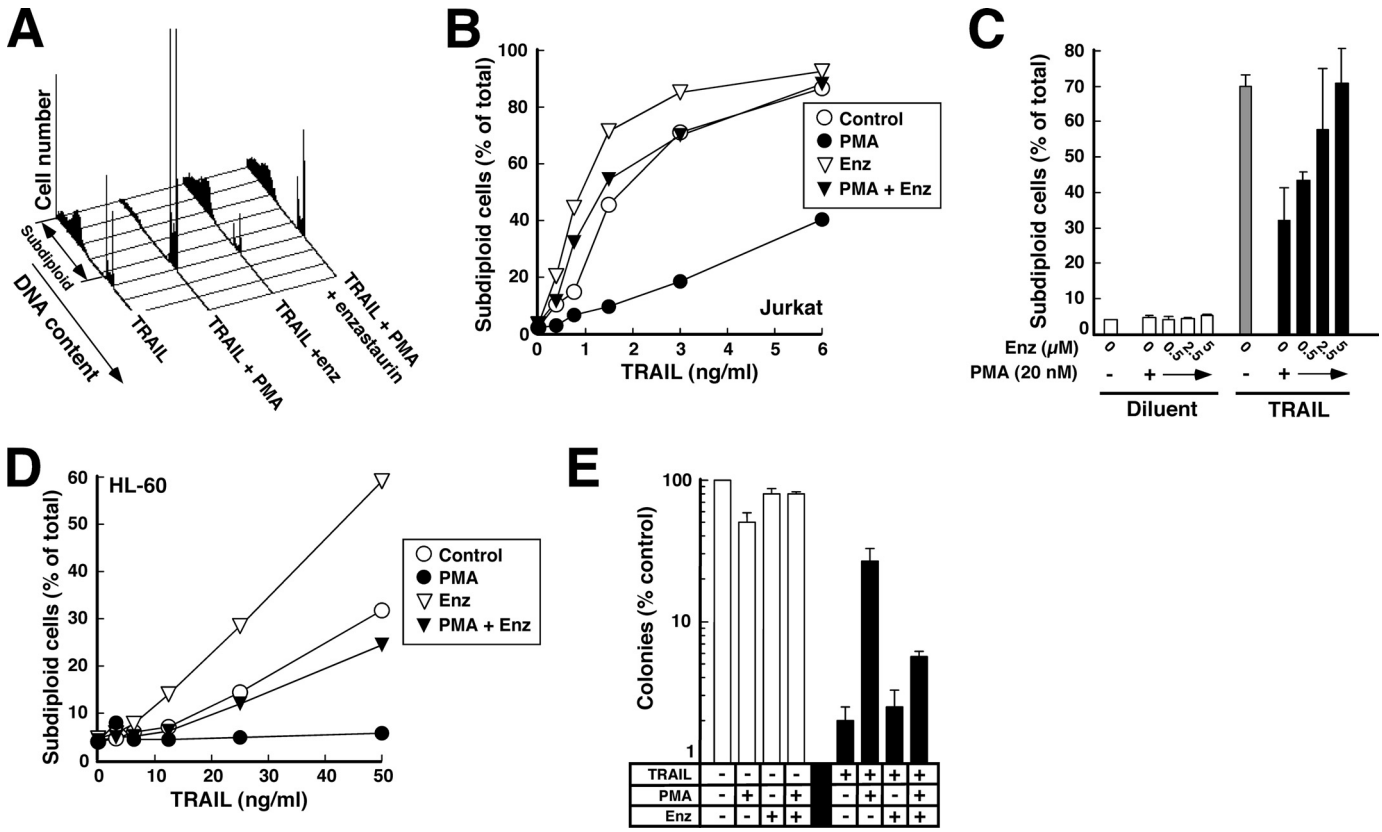

FIGURE 5. **Enzastaurin inhibits the effect of PMA on TRAIL-induced apoptosis.** *A,* after a 5-min pretreatment with 20 nM PMA or diluent (0.04% ethanol) and 10 μM enzastaurin (*Enz*) or diluent (0.02% DMSO), Jurkat cells were treated for 6 h with 3 ng/ml TRAIL, stained with PI, and analyzed by flow microfluorimetry. *B,* results from samples in *A* and additional samples from the same experiment. *C,* after a 5-min pretreatment with 20 nM PMA or diluent and the indicated concentration of enzastaurin or diluent, Jurkat cells were treated for 4 h with 6 ng/ml TRAIL, stained with PI, and analyzed by flow microfluorimetry. *Error bars,* ± S.D. of three independent experiments. *D,* after a 5-min pretreatment with 20 nM PMA or diluent (0.04% ethanol) and 10 μM enzastaurin or diluent (0.02% DMSO), HL-60 cells were treated for 4 h with the indicated concentration of TRAIL, stained with PI, and analyzed by flow microfluorimetry. *E,* after a 5-min pretreatment with 2 nM PMA or diluent and 10 μM enzastaurin or diluent, HL-60 cells were treated for 4 h with 25 ng/ml TRAIL, washed, diluted into 0.3% agar, and allowed to form colonies. *Error bars,* ± S.D. of quadruplicate samples.

transfected with PKCα shRNA (Fig. 3*B* and supplemental Fig. S2). PKCβ shRNA induced an even more dramatic effect (Fig. 3, *B* and *C,* and supplemental Fig. S2). Although there was little effect on apoptosis in the absence of PMA, the effect of PMA on death receptor-initiated apoptosis was severely blunted (Fig. 3, *B* and *C,* and supplemental Fig. S2), raising the possibility that PKCβ plays a major role in mediating the effect of PMA on death ligand-induced apoptosis.

PKCβ Inhibitor Enzastaurin Also Reverses the Effect of PMA—To further examine the role of PKCβ in death ligand-induced apoptosis, we evaluated the effects of enzastaurin, a small molecule PKCβ inhibitor that is currently undergoing clinical testing in diabetes and cancer (63–67). Initial experiments examined 10 μM enzastaurin, a concentration previously shown to suppress PMA-induced substrate phosphorylation in PKCβ-expressing U937 cells (68). As was the case with PKCβ shRNA, enzastaurin by itself did not induce apoptosis under the conditions of these assays but markedly blunted the effects of PMA on CH-11-induced apoptosis in Jurkat cells (Fig. 4, *A* and *B,* and supplemental Fig. S3). This sensitizing effect was seen at enzastaurin concentrations as low as 0.5 μM and was almost maximal at 5 μM (Fig. 4*C*), a concentration range that inhibits PKC substrate phosphorylation in cells (Fig. 4*D*) (68), diminishes activation-associated PKCβ down-regulation (Fig. 4*D*), and is sustainable in patients (64). Consistent with our previous results, PMA inhibited FADD recruitment to Fas, and enzastaurin mitigated this inhibition (Fig. 4*E*). As a result, enzastaurin facilitated CH-11-induced caspase 8 activation and subsequent downstream events in the presence of PMA (Fig. 4*F*).

Our previous results demonstrated that PMA protects Jurkat cells from the cytotoxicity of TRAIL, CH-11, and Fas ligand but not apoptosis induced through the mitochondrial pathway by camptothecin or etoposide (33), raising the possibility that PKC plays a specific role in modulating the death receptor pathway. Consistent with this possibility, treatment with enzastaurin had no effect on the induction of apoptosis by etoposide, staurosporine, or camptothecin (Fig. 4*G*).

Recent results have suggested that enzastaurin inhibits GSK3β in addition to PKCβ (69).[5] To assess whether the effects of enzastaurin were mediated by GSK3β, the ability of the GSK3β inhibitor LY2064827 to blunt the effects of PMA was assessed. As indicated in supplemental Fig. S4*A*, LY2064827 did little to reverse the effect of PMA on CH-11-induced killing. In contrast, 3-(1-(3-imidazol-1-ylpropyl)-1*H*-indol-3-yl)-4-anilino-1*H*-pyrrole-2,5-dione, a PKCβ inhibitor that is only dis-

[5] Eli Lilly Clinical Investigator Brochure for LY317615; D. D. Billadeau, unpublished observations.

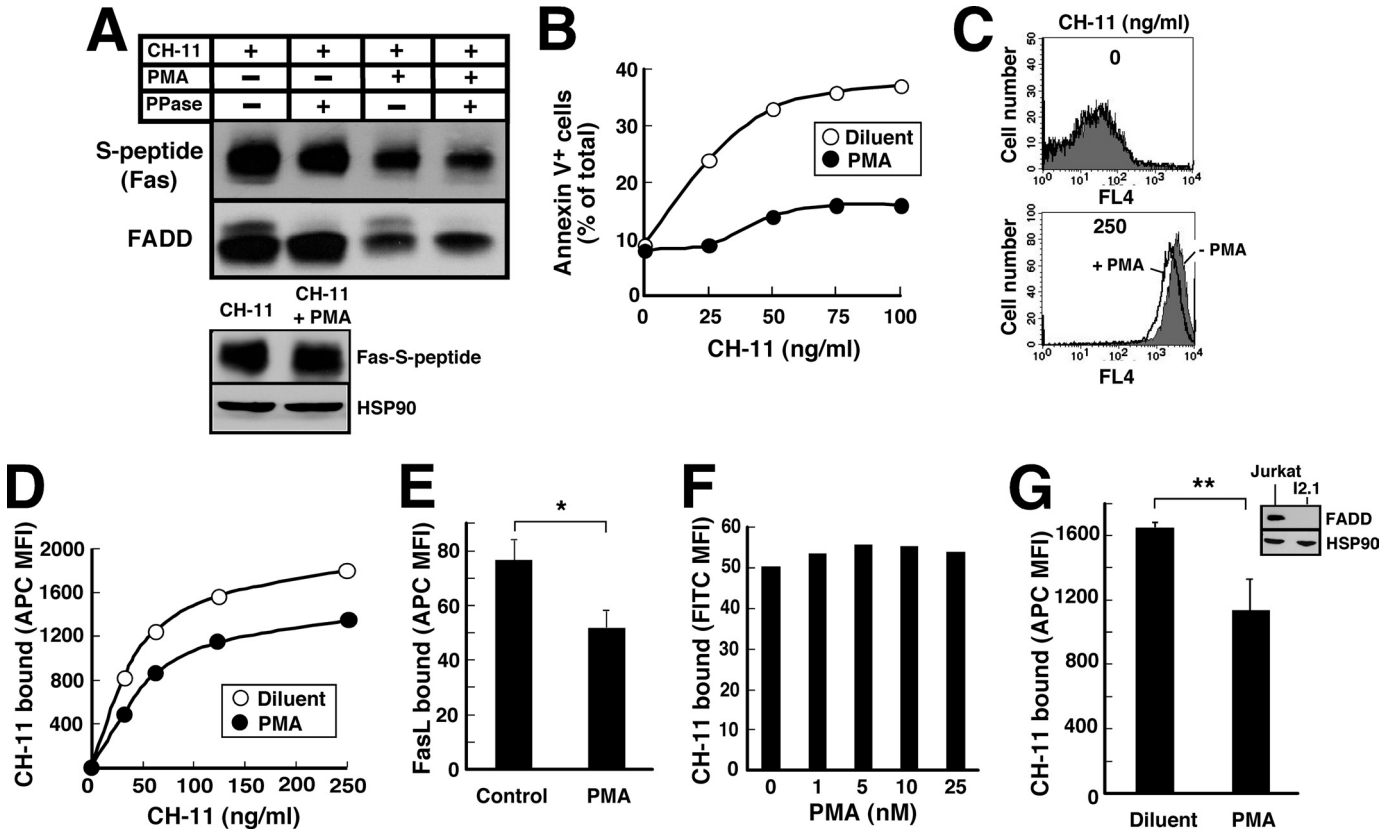

FIGURE 6. **PMA decreases the binding of Fas agonistic antibody and FasL.** *A,* after aliquots containing 5×10^7 JFSD9 cells (Fas-deficient cells reconstituted with Fas-S peptide) were incubated with 500 ng/ml CH-11 for 90 min in the absence or presence of 20 nM PMA, lysates were prepared as described under "Experimental Procedures." Half of each lysate was treated with λ-phosphatase (*PPase*) at 30 °C for 30 min. The Fas DISC was then pulled down with rabbit anti-mouse IgM and protein G-Sepharose as described previously (33). After SDS-PAGE, samples were blotted with mouse monoclonal anti-S-peptide and anti-FADD antibodies. *Lower panel,* cell lysates. HSP90 served as a loading control. *B,* after JFSD9 cells were treated for 5 h with the indicated concentration of CH-11 in the absence or presence of 20 nM PMA, apoptotic cells were quantified by annexin-V staining. *C,* Jurkat cells were treated with diluent (*top*) or 250 ng/ml CH-11 (*bottom*) without (*gray*) or with 20 nM PMA (*solid black line*) for 90 min at 37 °C, chilled, washed twice with ice-cold PBS, stained with APC-conjugated anti-mouse IgM, fixed, and analyzed by flow cytometry. *D,* summary of mean fluorescence intensity (*MFI*) obtained from samples in *C* and additional samples in the same experiment. *E,* Jurkat cells were treated with 400 ng/ml FLAG-tagged FasL + 1 μg/ml monoclonal anti-FLAG antibody (M2) for 90 min at 37 °C, chilled, washed twice with ice-cold PBS, stained with Alexa Fluor 647-conjugated anti-mouse IgG on ice for 1 h, fixed, and subjected to flow cytometry. *Error bars,* ± S.D. of three independent experiments. *, $p = 0.001$. *F,* Jurkat cells were treated with the indicated concentration of PMA at 37 °C for 90 min, chilled, washed, incubated with 250 ng/ml CH-11 on ice for 1 h, washed, stained with fluorescein isothiocyanate (*FITC*)-conjugated anti-mouse IgM on ice for 1 h, washed, fixed, and analyzed by flow cytometry. *G,* after I2.1 cells were treated with 125 ng/ml CH-11 in the absence or presence of 20 nM PMA for 90 min at 37 °C, bound CH-11 was assayed as detailed in *C. Error bars,* mean ± S.D. of three independent experiments. **, $p = 0.024$. *Inset,* whole cell lysates from Jurkat (*lane 1*) or I2.1 cells (*lane 2*) were probed with antibodies to FADD and, as a loading control, HSP90.

tantly related to enzastaurin, reversed the effects of PMA (supplemental Fig. S4*B*), albeit somewhat less potently than enzastaurin. These results suggest that enzastaurin, like PKCβ shRNA, is exerting its effects through inhibition of PKCβ.

In further experiments, enzastaurin also facilitated TRAIL-induced apoptosis in Jurkat cells (Fig. 5, *A* and *B*). This sensitizing effect was again observed at concentrations as low as 0.5 μM and was maximal at 5 μM (Fig. 5*C*). Similar sensitization was observed in HL-60 cells (Fig. 5*D*). Consistent with these results, enzastaurin also mitigated the effects of PMA as assessed by colony forming assays in the latter system (Fig. 5*E*).

PMA Diminishes Cell Surface Death Receptors —Previous experiments showing that treatment of cells with PMA interrupts death ligand-induced killing by disrupting recruitment of FADD to death receptors (32–34) raised the possibility that PMA might be inducing phosphorylation of death receptors or FADD. Preliminary experiments failed to demonstrate a PMA-induced change in FADD subcellular distribution[6] or increase in FADD phosphorylation (supplemental Fig. S5*A*). In contrast, PMA enhanced phosphorylation of tagged Fas (supplemental Fig. S5*B*). Mass spectrometry tentatively identified six phosphorylation sites (supplemental Fig. S5, *C–E*). Although Thr^{198} of Fas is a weak consensus PKC phosphorylation site, phosphorylation of Thr^{198} was not detected in multiple separate mass spectrometry experiments. Additional studies demonstrated that mutation of these putative phosphorylation sites to alanine singly (supplemental Fig. S6) or in combination (supplemental Fig. S7) failed to affect the ability of PMA to diminish FADD recruitment and inhibit Fas-mediated apoptosis. Accordingly, further experiments focused on other potential mechanisms by which PMA could affect Fas signaling.

To examine cell surface Fas levels, we initially transfected JM14A5 cells, a Jurkat variant that lacks cell surface Fas (45) and

[6] X. W. Meng and S. H. Kaufmann, unpublished observations.

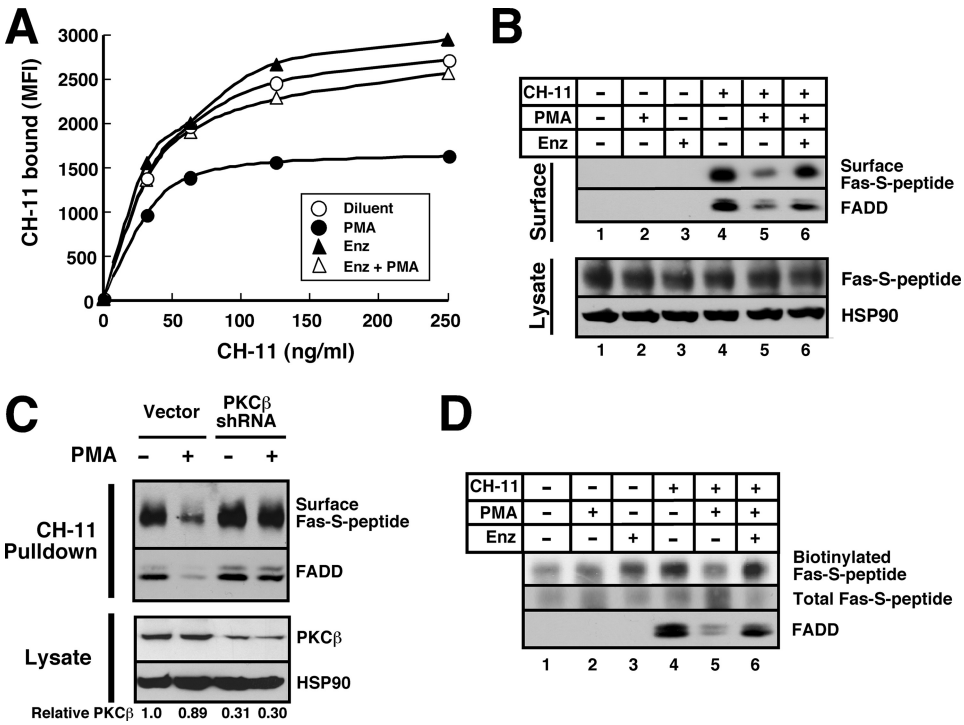

FIGURE 7. **PMA-induced attenuation of cell surface Fas is reversed by enzastaurin and PKCβ shRNA.** *A,* following pretreatment with 10 μM enzastaurin (*Enz*) or diluent for 30 min, Jurkat cells were incubated with CH-11 in the absence or presence of 20 nM PMA for additional 90 min at 37 °C and then stained with APC-conjugated anti-mouse IgM on ice as described the legend to Fig. 6*C*. *MFI,* mean fluorescence intensity. *B,* aliquots containing 5×10^7 JFSD9 cells were pretreated with diluent or 10 μM enzastaurin for 30 min and then incubated with 500 ng/ml CH-11 in the absence or presence of 20 nM PMA for 90 min at 37 °C. Lysates were prepared as described under "Experimental Procedures." Fas bound to CH-11 on the cell surface was recovered with anti-mouse IgM coupled to protein G-Sepharose. Immunoprecipitates were probed with antibodies to S peptide and FADD. *Bottom panel,* cell lysates from same cells. *C,* 48 h after JFSD9 cells were transfected with empty vector or PKCβ shRNA, cells were treated with 500 ng/ml CH-11 in the absence or presence of PMA. After cells were chilled and washed, CH-11 pulldowns prepared as described for Fig. 6*A* (*top*) and cell lysates (*bottom*) were probed with antibodies to the indicated antigens. HSP90 served as a loading control. *Numbers below lanes*, relative PKCβ signal of lysates after correction for HSP90 content. *D,* aliquots containing 5×10^7 JFSD9 cells were pretreated with diluent or 10 μM enzastaurin for 30 min and then incubated with 500 ng/ml CH-11 in the absence or presence of 20 nM PMA for 90 min at 37 °C. After cells were rapidly chilled on ice, cell surface proteins were biotinylated for 1 h at 4 °C as described under "Experimental Procedures." Following preparation of cell lysates, total cellular Fas-S peptide was recovered on beads containing anti-S peptide antibody (clone 6.2) coupled to protein G-Sepharose. After washing, bound proteins were subjected to SDS-PAGE and blotted with peroxidase-coupled streptavidin (*top*) for cell surface Fas, S peptide antibody (*middle,* for total Fas), or FADD (*bottom*).

is resistant to CH-11 (45, 53), with Fas tagged at its C terminus with S peptide. Control experiments demonstrated that Fas-S peptide signals like endogenous Fas (Fig. 6, *A* and *B*). In particular, treatment of reconstituted cells with CH-11 induced binding of FADD to Fas-S peptide (Fig. 6*A*, *upper panel, lane 1*) and subsequent apoptosis (Fig. 6*B*). In further experiments, cells expressing Fas-S peptide were treated with CH-11 agonistic anti-Fas antibody for 90 min in the absence and presence of PMA and then lysed so that CH-11-bound Fas and FADD could be recovered by immunoprecipitation.[7] Results of this analysis demonstrated that less Fas was recovered with CH-11 when the incubation was performed in the presence of PMA (Fig. 6*A*, *lanes 3* and *4 versus lane 1*). Importantly, the total amount of Fas detectable by blotting whole cell lysates with anti-S peptide antibody did not change (Fig. 6*A*, *lower panel*).

Subsequent experiments sought to extend these findings to endogenous untagged death receptors. Because of concern that anti-Fas antibodies can yield spurious results on immunoblots, alternative techniques were applied. In one line of experiments, parental Jurkat cells were incubated for 90 min with increasing CH-11 concentrations in the absence or presence of PMA; and cell surface antibody was subsequently detected by staining with APC-conjugated anti-mouse IgM at 4 °C followed by flow cytometry. Consistent with the results observed in transfected cells (Fig. 6*A*), less CH-11 was detectable on the cell surface when the incubation was performed in the presence of PMA (Fig. 6, *C* and *D*). Similarly, when parental Jurkat cells were treated with FasL in the absence and presence of PMA, less cell surface FasL was detected in the presence of PMA (Fig. 6*E*). Treatment with PMA alone at 37 °C for 90 min failed to alter the amount of CH-11 subsequently bound at 4 °C (Fig. 6*F*), suggesting that both PMA and ligand must be present in order for the effect of PMA to be detectable. When this effect of PMA and ligand on cell surface Fas was assessed in I2.1 cells, a Jurkat variant that lacks FADD and is resistant to Fas-mediated apoptosis (44, 45), decreased cell surface death receptor was again observed (Fig. 6*G*), indicating that the effect of PMA does not require Fas-FADD signaling. Collectively, these results suggest that PMA is diminishing Fas-mediated apoptosis, at least in part, by decreasing the amount of cell surface receptor available for ligand-induced activation.

Enzastaurin or PKCβ shRNA Increases Cell Surface Fas—In view of the ability of enzastaurin to reverse the effects of PMA on Fas-mediated apoptosis (Fig. 4), we next examined the ability of enzastaurin to reverse PMA-induced Fas down-regulation. When enzastaurin was added 30 min prior to CH-11 and PMA, subsequent flow cytometry demonstrated that enzastaurin restored the levels of CH-11 on the cell surface (Fig. 7*A*).

Similar effects of enzastaurin were observed using two additional approaches. In the first, cells expressing Fas-S peptide were treated with CH-11 for 90 min at 37 °C in the absence or presence of PMA and/or enzastaurin and then lysed so that

[7] This experiment and subsequent experiments analyzing cell surface death receptors were performed in the presence of 5 μM *N*-(2-quinolyl)-L-valyl-L-aspartyl-(2,6-difluorophenoxy) methyl ketone (95), a broad spectrum caspase inhibitor, to ensure that the results were not a reflection of caspase activation and/or subsequent apoptotic changes.

CH-11-bound Fas could be immunoprecipitated and probed with anti-S peptide antibody. As shown in Fig. 7*B*, PMA diminished the amount of Fas-S peptide bound to CH-11; and enzastaurin reversed this effect. PKCβ shRNA likewise restored the binding of CH-11 to Fas-S peptide in the presence of PMA (Fig. 7*C*).

In the second approach, cells expressing Fas-S peptide were treated with CH-11 in the absence or presence of PMA and/or enzastaurin for 90 min at 37 °C and then cooled to 4 °C. After cell surface proteins were biotinylated using cell-impermeable reagents (70, 71), total cellular Fas-S peptide was pulled down, subjected to SDS-PAGE, and probed with peroxidase-coupled streptavidin. Results of this analysis demonstrated that the amount of Fas accessible for biotinylation on the cell surface was markedly diminished after treatment with PMA (Fig. 7*D*, *lanes 4* and *5*); and this effect was again reversed by enzastaurin (Fig. 7*D*, *lane 6*). Collectively, the results in Fig. 7 using three independent methods suggest that enzastaurin or PKCβ shRNA is reversing the effects of PMA by preventing a PMA-induced decrease in cell surface Fas.

PMA Diminishes Fas Trafficking to the Cell Surface—Previous studies have demonstrated that PMA stimulates clathrin-mediated endocytosis of a number of cell surface receptors, including the transferrin receptor and epidermal growth factor receptor (72, 73). Consistent with these results, transfection with the C-terminal domain of the adapter protein AP-180 (74) or with dominant negative Eps-15 (75), two constructs that have previously been reported to inhibit clathrin-mediated uptake, inhibited PMA-induced loss of the transferrin receptor on the surface of Jurkat cells (supplemental Fig. S8*A*, *upper panel*). In contrast, these constructs had little effect on PMA-induced loss of CH-11 binding (supplemental Fig. S8*A*, *lower panel*). Likewise, mutation of Fas Tyr^{291} to Phe, a change reported to inhibit clathrin-mediated Fas internalization in some cells (21), had no effect on the PMA-induced decrease in CH-11 cell surface binding in Jurkat cells (supplemental Fig. S8*B*). Collectively, these results suggested that PMA is modulating cell surface death receptors by a process other than clathrin-mediated endocytosis.

Further examination of Fig. 7*D* indicated that more Fas-S peptide was detected on the cell surface in the presence of CH-11 than in its absence (Fig. 7*D*, *lanes 4* and *1*), raising the possibility that agonistic anti-Fas antibody is trapping the death receptor as it traffics to the cell surface. In further support of this hypothesis, cells incubated with CH-11 for increasing lengths of time were observed to have more cell surface Fas-S peptide accessible for biotinylation by cell-impermeable reagents (Fig. 8*A*, *lanes 1–5*). In contrast, treatment with CH-11 + PMA did not result in an increase in cell surface Fas (Fig. 8*A*, *lanes 6–10*). Similar results were observed when cells were stained with CH-11 at 37 °C for increasing lengths of time, cooled to 4 °C, stained with APC-conjugated secondary antibody, and analyzed by flow cytometry (Fig. 8*B*). Collectively, these results suggest that PMA is inhibiting ligand-induced accumulation of cell surface death receptor.

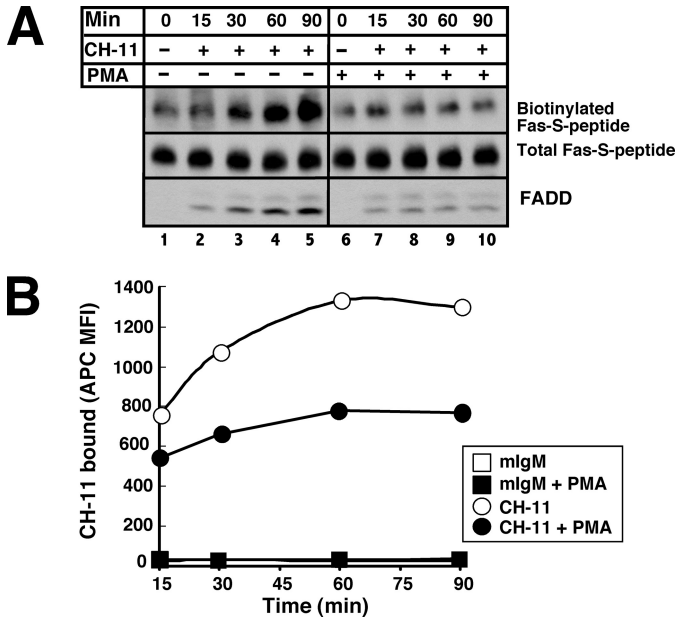

FIGURE 8. **PMA inhibits Fas trafficking to cell surface.** *A*, JFSD9 cells (reconstituted with Fas-S peptide) were treated with 500 ng/ml CH-11 (*lanes 2–5* and *7–10*) for the indicated lengths of time in the absence (*lanes 2–5*) or presence (*lanes 7–10*) of 20 nM PMA. For the 0-min time point, cells were treated with diluent (*lane 1*) or PMA for 90 min (*lane 6*). After cell surface proteins were biotinylated and cell lysates were prepared, S peptide-tagged Fas was recovered with anti-S peptide antibody coupled to protein G-agarose. Immunoprecipitates were probed with peroxidase-coupled streptavidin (*top*, cell surface Fas), anti-S peptide antibody (*middle*, total cellular Fas), or anti-FADD antibody. *B*, after Jurkat cells were treated with 250 ng/ml CH-11 (*circles*) or control IgM (*squares*) for the indicated length of time in the absence (*open symbols*) or presence (*closed symbols*) of 20 nM PMA, cells were cooled, washed labeled with APC-conjugated anti-mouse IgM, and analyzed as described in the legend to Fig. 6*C*. *MFI*, mean fluorescence intensity.

Enzastaurin Enhances TRAIL-induced Apoptosis in the Absence of PMA Treatment—Classical PKC isoforms are activated, in part, by phospholipase Cγ-mediated production of diacylglycerol after growth factor receptor ligation (61, 76). Further examination of Fig. 7, *A* and *D*, indicated that enzastaurin induced a slight but reproducible increase in cell surface Fas in the absence of PMA. Likewise, enzastaurin appeared to increase CH-11- and TRAIL-induced apoptosis in the absence of PMA (Fig. 4*B*, Fig. 5, *B* and *D*, and supplemental Fig. S3). These observations raised the possibility that tonic signaling by PKCβ, which is known to occur in a number of neoplasms (77–80), might contribute to death ligand resistance even in the absence of PMA. Consistent with this possibility, PKCβ shRNA enhanced TRAIL-induced apoptosis in T98G cells (Fig. 9*A*). In further experiments (Fig. 9, *B–D*), enzastaurin also enhanced the amount of TRAIL bound to the cell surface and its ability to induce apoptosis in this cell line. In addition, enzastaurin enhanced the antiproliferative effects of TRAIL (Fig. 9*E*) or agonistic anti-DR5 antibodies (Fig. 9*F*) in clonogenic assays. Enhanced antiproliferative effects were likewise observed when HeLa cervical cancer and HCT116 colon cancer cells were treated with TRAIL and enzastaurin compared with TRAIL alone (supplemental Fig. S9).

To rule out the possibility that these effects were unique to tissue culture cell lines, we also examined the ability of enzastaurin to enhance TRAIL-induced apoptosis in human acute

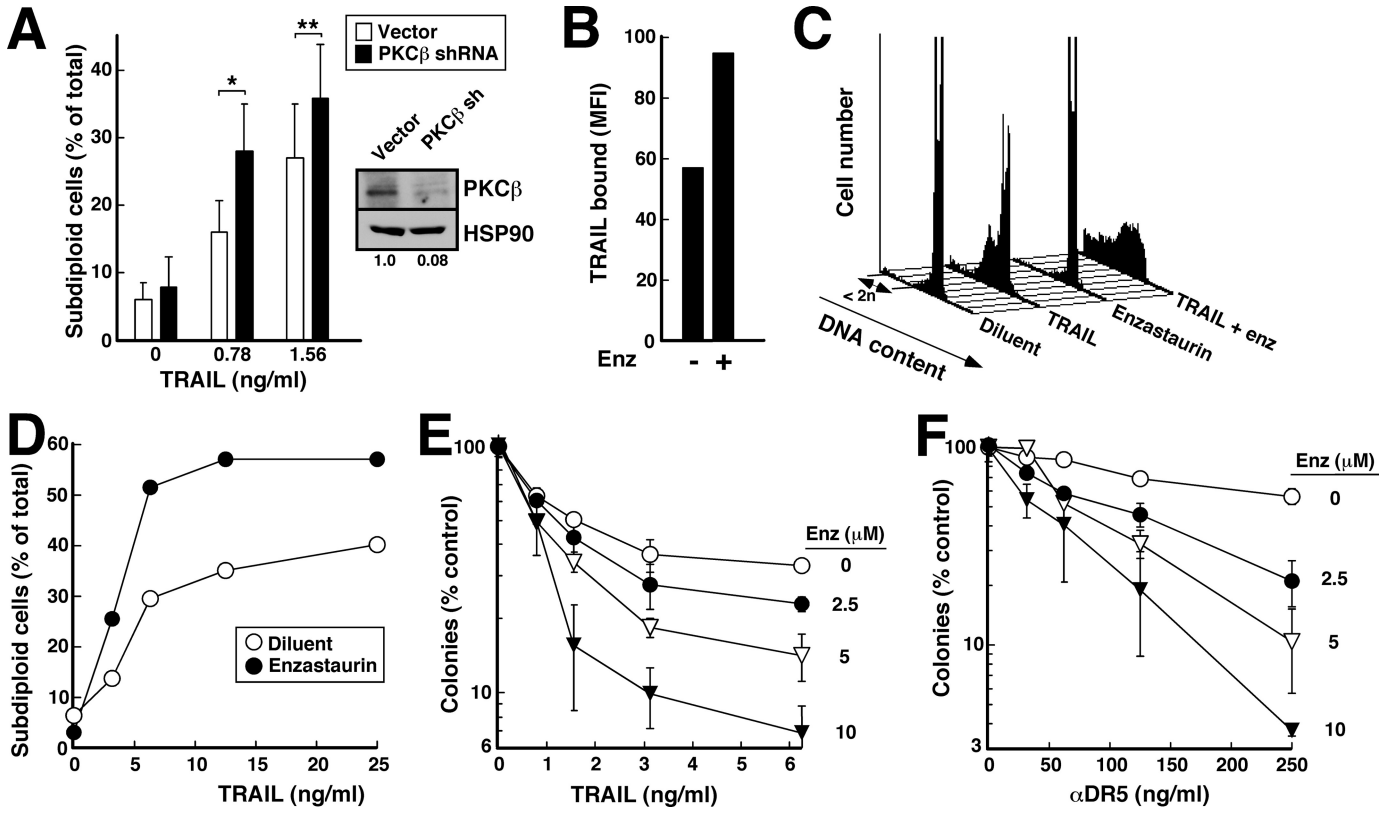

FIGURE 9. **Enzastaurin enhances TRAIL-induced apoptosis in the absence of PMA.** *A,* 72 h after transfection with PKCβ shRNA plasmid or empty vector, T98G cells were harvested for immunoblotting (*inset*) or treated for 4 h with the indicated TRAIL concentration. Because T98G cells do not bind annexin V, samples were stained with propidium iodide in buffer D and subjected to flow cytometry to assess DNA content. *Error bars*, $\pm$ S.D. of four independent experiments. * and **, $p = 0.003$ and 0.009 by two-tailed paired *t* test. *B,* T98G cells were treated with 400 ng/ml FLAG-tagged TRAIL + 1 μg/ml murine anti-FLAG antibody (clone M2) for 90 min in the absence or presence of 10 μM enzastaurin (*Enz*). At the completion of the incubation, cells were cooled to 4 °C, incubated for 45 min with Alexa Fluor647-coupled anti-mouse IgG, and examined by flow microfluorimetry. *C,* T98G cells were incubated for 4 h with 6.25 ng/ml TRAIL in the absence or presence of 10 μM enzastaurin. At the completion of the incubation, cells were stained with propidium iodide and subjected to flow microfluorimetry. *D,* summary of results from *B* and additional samples in the same experiment. *E* and *F,* T98G were incubated for 4 h with the indicated concentrations of TRAIL (*E*) or agonistic anti-DR5 antibody (*F*) in the absence or presence of the indicated concentration of enzastaurin. At the completion of the incubation, cells were washed and then incubated in drug-free medium until colonies formed. All values are normalized to cells treated with diluent alone (no enzastaurin or TRAIL). Because enzastaurin has no effect by itself under the conditions of these assays, its ability to enhance the effects of TRAIL meets the definition of synergy (82). *Error bars,* $\pm$ S.D. of triplicate aliquots. *MFI,* mean fluorescence intensity.

myelogenous leukemia isolates. Preliminary studies established that these cells express abundant levels of PKCβ (Fig. 10*A*). Although enzastaurin by itself had little effect on these cells (Fig. 10*B, inset*), it nonetheless enhanced TRAIL-induced apoptosis (Fig. 10, *B* and *C*). Formal mathematical analysis using the median effect method of Chou and Talalay (81), a standard approach to assessing the effects of combined treatments (82), indicated that the effects were more than additive at the vast majority of data points in the nine acute myelogenous leukemia samples, as indicated by the combination index that was <1 (Fig. 10*D*).

DISCUSSION

Results of this study demonstrated that PMA enhances short term and long term survival of death ligand-treated cells and that these effects occur at low nanomolar PMA concentrations. In further experiments, these protective effects of PMA were inhibited by PKCβ shRNA or enzastaurin. In addition, PMA diminished the amount of cell surface death receptor, whereas PKCβ shRNA or enzastaurin reversed this effect. Collectively, these observations suggest that PMA and enzastaurin modulate the trafficking of Fas and DR5 to the cell surface, thereby affecting the amount of receptor available for ligation and the activation of the death receptor pathway. These observations have implications not only for current understanding of the death receptor pathway, but also potentially for the clinical development of death ligands as anticancer agents.

Although a number of previous studies reported that PMA can protect from death ligand-induced apoptosis, it was previously unclear whether cell death was delayed or abrogated. In this study, outgrowth assays (Fig. 1, *D* and *F*) as well as clonogenic assays (Fig. 1*H* and Fig. 5*E*) demonstrated that concurrent PMA treatment enhanced the number of cells that were able to survive and proliferate after TRAIL exposure. These results are consistent with scattered reports showing that proliferating cells, which often have activated PKCs, are less sensitive to TRAIL (83, 84) and that selection for TRAIL resistance yields cells with accelerated proliferation (85).

During the course of the studies on PMA-induced protection from death ligands, we also observed that the protective effects are close to maximal at PMA concentrations in the 1–2 nM range (Fig. 1, *B*, *E,* and *G*). Further experiments showed that a number of PKC isoforms are activated over this concentration range (Fig. 2). Although shRNA that selectively down-regulates

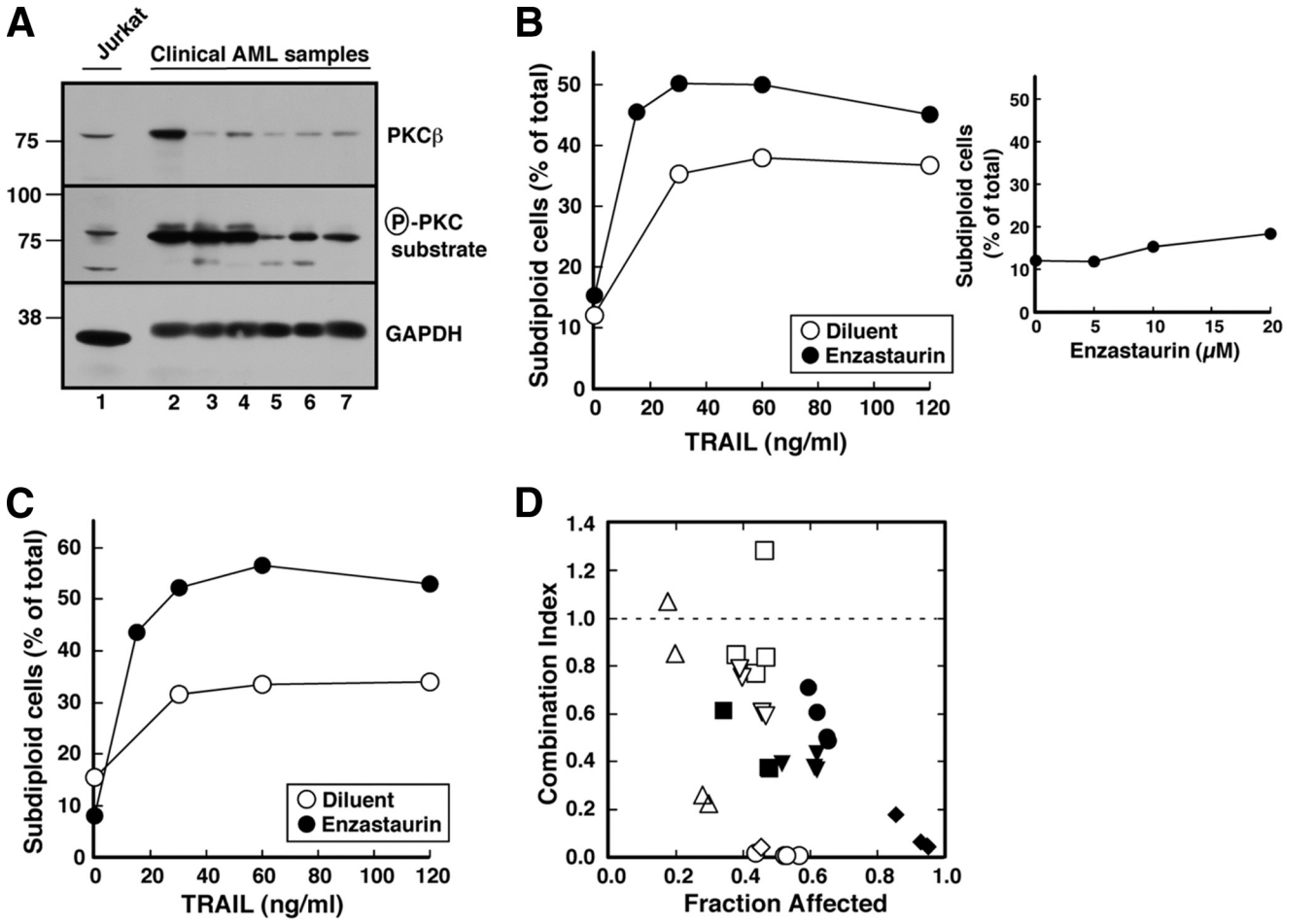

FIGURE 10. **Enzastaurin sensitizes clinical acute myelogenous leukemia samples to TRAIL.** *A,* in the absence of PMA stimulation, whole cell lysates from 5×10^5 log phase Jurkat cells (*lane 1*) or six freshly isolated acute myelogenous leukemia (*AML*) specimens (*lanes 2–7*) were subjected to SDS-PAGE, transferred to nitrocellulose, and probed with antibodies to the indicated antigen. *GADPH*, glyceraldehyde-3-phosphate dehydrogenase. *B* and *C,* freshly isolated mononuclear cells from two newly diagnosed acute myelogenous leukemia patients incubated for 24 h with the indicated concentration of TRAIL in the absence or presence of 10 μM enzastaurin. At the completion of the incubation, cells were washed in PBS, fixed in 50% ethanol, rehydrated, stained with propidium iodide, and subjected to flow microfluorimetry. Events with $<2n$ DNA content were counted as illustrated in Fig. 1*A* and Fig. 4*A*. *Inset* in *B,* cells treated for 24 h with the indicated concentrations of enzastaurin in the absence of TRAIL were stained and examined by flow microfluorimetry. *D,* combination index values (81) calculated from the data in *B* (*open diamonds*), *C* (*open circles*), and assays in samples from seven other acute myelogenous leukemia patients (*other symbols*) using an approach that renders the analysis equivalent to isobologram analysis (82). Note that a combination index <1.0 indicates synergy.

PKCε or PKCθ had little effect on PMA-induced protection, PKCα shRNA mitigated the effects of PMA to a limited extent, and PKCβ shRNA markedly diminished the effects of PMA (Fig. 3). Consistent with these results, the PKCβ inhibitor enzastaurin diminished the effects of PMA on DISC formation (Fig. 4*E*) and subsequent apoptosis (Fig. 4, *A*, *B,* and *F*).

In further experiments, three independent approaches detected fewer death receptors on the surfaces of cells treated with death ligand in the presence of PMA compared with its absence. First, in cells expressing epitope-tagged Fas, diminished receptor was pulled down with CH-11 in the presence of PMA (Fig. 6*A* and Fig. 7*B*). Second, when cell surface proteins were biotinylated and total cellular Fas was recovered using the epitope tag, less Fas was derivatized if the incubation included PMA (Fig. 7*D* and Fig. 8*A*). Finally, when cells were treated with death ligand at 37 °C, cooled to 4 °C, and reacted with fluorochrome-conjugated secondary antibodies, flow cytometry detected less endogenous Fas (Fig. 6, *C* and *D*, Fig. 7*A,* and Fig. 8*B*) or FasL (Fig. 6*E*) on the cell surface if the incubation included PMA. During the course of these studies we noted that the PMA-induced decrease in cell surface receptor appeared to be greater using the former two assays. In view of the fact that effects of PMA on cell surface ligand binding were somewhat less dramatic than the protection against death ligand-induced death (*cf.* Fig. 6, *B* and *D*), we cannot rule out the possibility that PKCβ is also involved in other changes that protect cells from death ligand-induced apoptosis. Although the reason for the quantitative difference between the assays is currently unknown, all three assays led to the conclusion that PMA is acting, at least in part, by regulating the number of cell surface death receptors.

PKC isoforms have previously been implicated in down-regulation of other types of cell surface receptors through enhanced receptor internalization (72). In contrast, results of this study failed to provide evidence for PMA-induced internalization of Fas. PMA did not stimulate clathrin-mediated Fas internalization, as indicated by (i) the inability of overexpressed c-AP180 or dominant negative Eps-15 to prevent the PMA-induced decrement in cell surface Fas (supplemental Fig. S8*A*) and (ii) the failure of the Fas Y291F mutation to mitigate the effects of

PMA (supplemental Fig. S8*B*). Moreover, the failure of PMA to cause a decrease in cell surface Fas over time (Fig. 8) argues against the possibility that PMA is accelerating a clathrin-independent internalization mechanism.

Instead, our observations suggest a model in which CH-11 is progressively trapping Fas as it spontaneously traffics to the Jurkat cell surface in a PKCβ-regulated manner. In particular, two independent lines of evidence (Fig. 8, *A* and *B*) demonstrate that cell surface Fas increases during time of exposure to agonistic antibody. Both experiments also show that PMA markedly diminishes this increase. These observations not only explain our prior observation that the amount of Fas DISC detectable in Jurkat cells increases progressively with time of death ligand incubation (33), but also provide an explanation for the ability of PMA to protect cells when added only 5 min before death ligands. Additional experiments demonstrated that the effects of PMA on cell surface Fas were reversed by PKCβ shRNA (Fig. 7*C*) or enzastaurin (Fig. 7, *A*, *B,* and *D*). To our knowledge, these experiments provide the first evidence that PKC plays an important role in trafficking of death receptors.

Previous studies have suggested the possibility that death receptor trafficking might be a regulated process. In particular, Bennett *et al.* (86) reported that DNA damage increases the amount of cell surface Fas in a p53-dependent manner. Our results complement and extend those of Bennett *et al.* (86) by (i) showing that trafficking of TRAIL receptors is also regulated (Fig. 9*B*), (ii) implicating PKC in this process, and (iii) demonstrating that the PKC-mediated process can be observed in cells that lack p53 (HL-60, Fig. 5, *D* and *E*), as well as cells that contain p53 (*e.g.* HCT116, supplemental Fig. S9).

Although enzastaurin is often described as a PKCβ-selective inhibitor (66, 87), the assignment of PKCβ as the isoform responsible for modulating death receptor trafficking must be viewed as tentative. Even though the concentrations of enzastaurin utilized in this study are therapeutically achievable (64) and are similar to those required to inhibit PMA-induced PKC substrate phosphorylation in cells expressing PKCβ (68), these effects are observed at concentrations where enzastaurin could conceivably inhibit other kinases (69), especially other PKC isoforms (63). On the other hand, the ability of another PKCβ-selective inhibitor (supplemental Fig. S4*B*) and PKCβ shRNA to mitigate the effects of PMA provides additional support for the view that PKCβ might play a major role in modulating death receptor trafficking.

In view of the fact that PKC isoforms are often activated by growth factor signaling, we asked whether enzastaurin might also modulate TRAIL signaling in the absence of PMA. Consistent with this possibility, enzastaurin enhanced TRAIL binding as well as TRAIL-induced antiproliferative effects in a number of tissue culture cell lines (Fig. 9 and supplemental Fig. S9). Moreover, enzastaurin synergistically enhanced TRAIL-induced apoptosis in clinical acute myelogenous leukemia isolates (Fig. 10). These results are consistent with the view that ongoing signaling might dampen the response to TRAIL even in the absence of exogenous phorbol esters. Further studies are required to determine the extent of this death ligand-inhibiting signaling in various preclinical and clinical settings as well as determine the effect of this signaling on the response to TRAIL and agonistic antibodies in the clinical setting.

Previous studies have indicated that the relationship between expression of TRAIL receptors and TRAIL sensitivity is complex. On the one hand, up-regulation of DR4 and/or DR5 after DNA damage (88, 89) or proteasome inhibition (90–92) is associated with enhanced TRAIL sensitivity. On the other hand, basal levels of expression of DR4 and DR5 levels have not always correlated with TRAIL sensitivity (93). This lack of correlation has previously been attributed to overexpression of decoy receptors, XIAP, antiapoptotic Bcl-2 family members, and/or c-FLIP (6, 9, 93) as well as post-translational modifications of DR4 and DR5 (19). The present results suggest that receptor trafficking also needs to be taken into account. In particular, basal measurements of cell surface DR4 or DR5 might not fully reflect the levels of receptor available at the cell surface upon prolonged ligand exposure. On the other hand, it is also important to emphasize that the present studies were all performed with cell lines that exhibit some degree of TRAIL sensitivity before treatment with PKCβ shRNA or enzastaurin. Based on the mechanism identified through this study, it is unclear whether enzastaurin or PKCβ shRNA would be able to overcome TRAIL resistance that results from overexpression of decoy receptors, c-FLIP, antiapoptotic Bcl-2 family members, or XIAP. Further study is required to address this issue.

In summary, the results of this study not only suggest that PKCβ mediates the effects of PMA on death receptor signaling but also demonstrate that these effects reflect an effect on death ligand trafficking. Whether enzastaurin, which enhances cell surface death receptors, will be a useful addition to death ligand treatment requires further preclinical and clinical investigation.

Acknowledgments—We thank Bill Karnes for initial aliquots of isoform-specific PKC antibodies; Guy Poirier, David Toft, and Andreas Strasser for antibodies; the Flow Cytometry and Optical Morphology Shared Resource of the Mayo Clinic Cancer Center for assistance with the flow cytometry; Greg Gores, Matthew Ames, and Larry Karnitz for discussion and encouragement; and Deb Strauss for editorial assistance.

REFERENCES

1. Ashkenazi, A., and Dixit, V. M. (1998) *Science* **281,** 1305–1308
2. Walczak, H., and Krammer, P. H. (2000) *Exp. Cell Res.* **256,** 58–66
3. Strasser, A., Jost, P. J., and Nagata, S. (2009) *Immunity* **30,** 180–192
4. Nagata, S. (1997) *Cell* **88,** 355–365
5. Wajant, H. (2006) *Cancer Treat. Res.* **130,** 141–165
6. Thorburn, A., Behbakht, K., and Ford, H. (2008) *Drug Resist. Updat.* **11,** 17–24
7. Johnstone, R. W., Frew, A. J., and Smyth, M. J. (2008) *Nat. Rev. Cancer* **8,** 782–798
8. Falschlehner, C., Schaefer, U., and Walczak, H. (2009) *Immunology* **127,** 145–154
9. Ashkenazi, A. (2008) *Nat. Rev. Drug Discovery* **7,** 1001–1012
10. Kischkel, F. C., Hellbardt, S., Behrmann, I., Germer, M., Pawlita, M., Krammer, P. H., and Peter, M. E. (1995) *EMBO J.* **14,** 5579–5588
11. Siegel, R. M., Martin, D. A., Zheng, L., Ng, S. Y., Bertin, J., Cohen, J., and Lenardo, M. J. (1998) *J. Cell Biol.* **141,** 1243–1253
12. Scott, F. L., Stec, B., Pop, C., Dobaczewska, M. K., Lee, J. J., Monosov, E., Robinson, H., Salvesen, G. S., Schwarzenbacher, R., and Riedl, S. J. (2009)

Nature **457,** 1019–1022
13. Muzio, M., Chinnaiyan, A. M., Kischkel, F. C., O'Rourke, K., Shevchenko, A., Ni, J., Scaffidi, C., Bretz, J. D., Zhang, M., Gentz, R., Mann, M., Krammer, P. H., Peter, M. E., and Dixit, V. M. (1996) *Cell* **85,** 817–827
14. Kischkel, F. C., Lawrence, D. A., Tinel, A., LeBlanc, H., Virmani, A., Schow, P., Gazdar, A., Blenis, J., Arnott, D., and Ashkenazi, A. (2001) *J. Biol. Chem.* **276,** 46639–46646
15. Boatright, K. M., Renatus, M., Scott, F. L., Sperandio, S., Shin, H., Pedersen, I. M., Ricci, J. E., Edris, W. A., Sutherlin, D. P., Green, D. R., and Salvesen, G. S. (2003) *Mol. Cell* **11,** 529–541
16. Medema, J. P., Scaffidi, C., Kischkel, F. C., Shevchenko, A., Mann, M., Krammer, P. H., and Peter, M. E. (1997) *EMBO J.* **16,** 2794–2804
17. Chang, D. W., Xing, Z., Capacio, V. L., Peter, M. E., and Yang, X. (2003) *EMBO J.* **22,** 4132–4142
18. Hughes, M. A., Harper, N., Butterworth, M., Cain, K., Cohen, G. M., and MacFarlane, M. (2009) *Mol. Cell* **35,** 265–279
19. Wagner, K. W., Punnoose, E. A., Januario, T., Lawrence, D. A., Pitti, R. M., Lancaster, K., Lee, D., von Goetz, M., Yee, S. F., Totpal, K., Huw, L., Katta, V., Cavet, G., Hymowitz, S. G., Amler, L., and Ashkenazi, A. (2007) *Nat. Med.* **13,** 1070–1077
20. Ashkenazi, A., and Dixit, V. M. (1999) *Curr. Opin. Cell Biol.* **11,** 255–260
21. Lee, K. H., Feig, C., Tchikov, V., Schickel, R., Hallas, C., Schütze, S., Peter, M. E., and Chan, A. C. (2006) *EMBO J.* **25,** 1009–1023
22. Schütze, S., Tchikov, V., and Schneider-Brachert, W. (2008) *Nat. Rev. Mol. Cell Biol.* **9,** 655–662
23. Guicciardi, M. E., and Gores, G. J. (2009) *FASEB J.* **23,** 1625–1637
24. Alappat, E. C., Feig, C., Boyerinas, B., Volkland, J., Samuels, M., Murmann, A. E., Thorburn, A., Kidd, V. J., Slaughter, C. A., Osborn, S. L., Winoto, A., Tang, W. J., and Peter, M. E. (2005) *Mol. Cell* **19,** 321–332
25. Werner, M. H., Wu, C., and Walsh, C. M. (2006) *Cell Cycle* **5,** 2332–2338
26. Yu, J. W., and Shi, Y. (2008) *Oncogene* **27,** 6216–6227
27. Chang, D. W., Xing, Z., Pan, Y., Algeciras-Schimnich, A., Barnhart, B. C., Yaish-Ohad, S., Peter, M. E., and Yang, X. (2002) *EMBO J.* **21,** 3704–3714
28. Panner, A., James, C. D., Berger, M. S., and Pieper, R. O. (2005) *Mol. Cell. Biol.* **25,** 8809–8823
29. Ueffing, N., Singh, K. K., Christians, A., Thorns, C., Feller, A. C., Nagl, F., Fend, F., Heikaus, S., Marx, A., Zotz, R. B., Brade, J., Schulz, W. A., Schulze-Osthoff, K., Schmitz, I., and Schwerk, C. (2009) *Blood* **114,** 572–579
30. Yu, J. W., Jeffrey, P. D., and Shi, Y. (2009) *Proc. Natl. Acad. Sci. U.S.A.* **106,** 8169–8174
31. McDonald, E. R., 3rd, and El-Deiry, W. S. (2004) *Proc. Natl. Acad. Sci. U.S.A.* **101,** 6170–6175
32. Gómez-Angelats, M., and Cidlowski, J. A. (2001) *J. Biol. Chem.* **276,** 44944–44952
33. Meng, X. W., Heldebrant, M. P., and Kaufmann, S. H. (2002) *J. Biol. Chem.* **277,** 3776–3783
34. Harper, N., Hughes, M. A., Farrow, S. N., Cohen, G. M., and MacFarlane, M. (2003) *J. Biol. Chem.* **278,** 44338–44347
35. Holmström, T. H., Schmitz, I., Söderström, T. S., Poukkula, M., Johnson, V. L., Chow, S. C., Krammer, P. H., and Eriksson, J. E. (2000) *EMBO J.* **19,** 5418–5428
36. Ito, T., Deng, X., Carr, B., and May, W. S. (1997) *J. Biol. Chem.* **272,** 11671–11673
37. Domina, A. M., Vrana, J. A., Gregory, M. A., Hann, S. R., and Craig, R. W. (2004) *Oncogene* **23,** 5301–5315
38. Busuttil, V., Bottero, V., Frelin, C., Imbert, V., Ricci, J. E., Auberger, P., and Peyron, J. F. (2002) *Oncogene* **21,** 3213–3224
39. Wajant, H. (2004) *Vitam. Horm.* **67,** 101–132
40. Hendrickson, A. W., Meng, X. W., and Kaufmann, S. H. (2008) *J. Clin. Invest.* **118,** 3582–3584
41. Reyland, M. E. (2009) *Front. Biosci.* **14,** 2386–2399
42. Mesner, P. W., Jr., Bible, K. C., Martins, L. M., Kottke, T. J., Srinivasula, S. M., Svingen, P. A., Chilcote, T. J., Basi, G. S., Tung, J. S., Krajewski, S., Reed, J. C., Alnemri, E. S., Earnshaw, W. C., and Kaufmann, S. H. (1999) *J. Biol. Chem.* **274,** 22635–22645
43. Hackbarth, J. S., Lee, S. H., Meng, X. W., Vroman, B. T., Kaufmann, S. H., and Karnitz, L. M. (2004) *BioTechniques* **37,** 835–839
44. Juo, P., Woo, M. S., Kuo, C. J., Signorelli, P., Biemann, H. P., Hannun, Y. A., and Blenis, J. (1999) *Cell Growth & Differ.* **10,** 797–804
45. Meng, X. W., Chandra, J., Loegering, D., Van Becelaere, K., Kottke, T. J., Gore, S. D., Karp, J. E., Sebolt-Leopold, J., and Kaufmann, S. H. (2003) *J. Biol. Chem.* **278,** 47326–47339
46. Pike, B. L., and Robinson, W. A. (1970) *J. Cell Physiol.* **76,** 77–84
47. Simonian, P. L., Grillot, D. A., and Nuñez, G. (1997) *Blood* **90,** 1208–1216
48. Meng, X. W., Lee, S. H., Dai, H., Loegering, D., Yu, C., Flatten, K., Schneider, P., Dai, N. T., Kumar, S. K., Smith, B. D., Karp, J. E., Adjei, A. A., and Kaufmann, S. H. (2007) *J. Biol. Chem.* **282,** 29831–29846
49. Dai, H., Meng, X. W., Lee, S. H., Schneider, P. A., and Kaufmann, S. H. (2009) *J. Biol. Chem.* **284,** 18311–18322
50. Nicoletti, I., Migliorati, G., Pagliacci, M. C., Grignani, F., and Riccardi, C. (1991) *J. Immunol. Methods* **139,** 271–279
51. Svingen, P. A., Tefferi, A., Kottke, T. J., Kaur, G., Narayanan, V. L., Sausville, E. A., and Kaufmann, S. H. (2000) *Clin. Cancer Res.* **6,** 237–249
52. Gomez, T. S., McCarney, S. D., Carrizosa, E., Labno, C. M., Comiskey, E. O., Nolz, J. C., Zhu, P., Freedman, B. D., Clark, M. R., Rawlings, D. J., Billadeau, D. D., and Burkhardt, J. K. (2006) *Immunity* **24,** 741–752
53. Eischen, C. M., Kottke, T. J., Martins, L. M., Basi, G. S., Tung, J. S., Earnshaw, W. C., Leibson, P. J., and Kaufmann, S. H. (1997) *Blood* **90,** 935–943
54. Kaufmann, S. H., Svingen, P. A., Gore, S. D., Armstrong, D. K., Cheng, Y. C., and Rowinsky, E. K. (1997) *Blood* **89,** 2098–2104
55. Smith, P. K., Krohn, R. I., Hermanson, G. T., Mallia, A. K., Gartner, F. H., Provenzano, M. D., Fujimoto, E. K., Goeke, N. M., Olson, B. J., and Klenk, D. C. (1985) *Anal. Biochem.* **150,** 76–85
56. Yu, C., Bruzek, L. M., Meng, X. W., Gores, G. J., Carter, C. A., Kaufmann, S. H., and Adjei, A. A. (2005) *Oncogene* **24,** 6861–6869
57. Kaufmann, S. H. (2001) *Anal. Biochem.* **296,** 283–286
58. English, D., and Andersen, B. R. (1974) *J. Immunol. Methods* **5,** 249–252
59. Ekert, P. G., Read, S. H., Silke, J., Marsden, V. S., Kaufmann, H., Hawkins, C. J., Gerl, R., Kumar, S., and Vaux, D. L. (2004) *J. Cell Biol.* **165,** 835–842
60. Nishizuka, Y. (1995) *FASEB J.* **9,** 484–496
61. Dempsey, E. C., Newton, A. C., Mochly-Rosen, D., Fields, A. P., Reyland, M. E., Insel, P. A., and Messing, R. O. (2000) *Am. J. Physiol. Lung Cell Mol. Physiol.* **279,** L429–L438
62. Parker, P. J., and Murray-Rust, J. (2004) *J. Cell Sci.* **117,** 131–132
63. Graff, J. R., McNulty, A. M., Hanna, K. R., Konicek, B. W., Lynch, R. L., Bailey, S. N., Banks, C., Capen, A., Goode, R., Lewis, J. E., Sams, L., Huss, K. L., Campbell, R. M., Iversen, P. W., Neubauer, B. L., Brown, T. J., Musib, L., Geeganage, S., and Thornton, D. (2005) *Cancer Res.* **65,** 7462–7469
64. Carducci, M. A., Musib, L., Kies, M. S., Pili, R., Truong, M., Brahmer, J. R., Cole, P., Sullivan, R., Riddle, J., Schmidt, J., Enas, N., Sinha, V., Thornton, D. E., and Herbst, R. S. (2006) *J. Clin. Oncol.* **24,** 4092–4099
65. Teicher, B. A. (2006) *Clin. Cancer Res.* **12,** 5336–5345
66. Herbst, R. S., Oh, Y., Wagle, A., and Lahn, M. (2007) *Clin. Cancer Res.* **13,** (suppl. 15), 4641S–4646S
67. Podar, K., Raab, M. S., Chauhan, D., and Anderson, K. C. (2007) *Expert Opin. Investig. Drugs* **16,** 1693–1707
68. Green, L. J., Marder, P., Ray, C., Cook, C. A., Jaken, S., Musib, L. C., Herbst, R. S., Carducci, M., Britten, C. D., Basche, M., Eckhardt, S. G., and Thornton, D. (2006) *Clin. Cancer Res.* **12,** 3408–3415
69. Fedorov, O., Marsden, B., Pogacic, V., Rellos, P., Müller, S., Bullock, A. N., Schwaller, J., Sundström, M., and Knapp, S. (2007) *Proc. Natl. Acad. Sci. U.S.A.* **104,** 20523–20528
70. Pelchen-Matthews, A., Armes, J. E., and Marsh, M. (1989) *EMBO J.* **8,** 3641–3649
71. Le Bivic, A., Sambuy, Y., Mostov, K., and Rodriguez-Boulan, E. (1990) *J. Cell Biol.* **110,** 1533–1539
72. Beguinot, L., Hanover, J. A., Ito, S., Richert, N. D., Willingham, M. C., and Pastan, I. (1985) *Proc. Natl. Acad. Sci. U.S.A.* **82,** 2774–2778
73. Doherty, G. J., and McMahon, H. T. (2009) *Annu. Rev. Biochem.* **78,** 857–902
74. Ford, M. G., Pearse, B. M., Higgins, M. K., Vallis, Y., Owen, D. J., Gibson, A., Hopkins, C. R., Evans, P. R., and McMahon, H. T. (2001) *Science* **291,** 1051–1055
75. Matharu, A. L., Mundell, S. J., Benovic, J. L., and Kelly, E. (2001) *J. Biol. Chem.* **276,** 30199–30207
76. Griner, E. M., and Kazanietz, M. G. (2007) *Nat. Rev. Cancer* **7,** 281–294

77. Shipp, M. A., Ross, K. N., Tamayo, P., Weng, A. P., Kutok, J. L., Aguiar, R. C., Gaasenbeek, M., Angelo, M., Reich, M., Pinkus, G. S., Ray, T. S., Koval, M. A., Last, K. W., Norton, A., Lister, T. A., Mesirov, J., Neuberg, D. S., Lander, E. S., Aster, J. C., and Golub, T. R. (2002) *Nat. Med.* **8,** 68–74
78. Koivunen, J., Aaltonen, V., and Peltonen, J. (2006) *Cancer Lett.* **235,** 1–10
79. Martiny-Baron, G., and Fabbro, D. (2007) *Pharmacol. Res.* **55,** 477–486
80. Abrams, S. T., Lakum, T., Lin, K., Jones, G. M., Treweeke, A. T., Farahani, M., Hughes, M., Zuzel, M., and Slupsky, J. R. (2007) *Blood* **109,** 1193–1201
81. Chou, T. C., and Talalay, P. (1984) *Adv. Enzyme Regul.* **22,** 27–55
82. Berenbaum, M. C. (1989) *Pharmacol. Rev.* **41,** 93–141
83. Qin, J. Z., Bacon, P. E., Chaturvedi, V., Bonish, B., and Nickoloff, B. J. (2002) *Exp. Dermatol.* **11,** 573–583
84. Behbakht, K., Qamar, L., Aldridge, C. S., Coletta, R. D., Davidson, S. A., Thorburn, A., and Ford, H. L. (2007) *Cancer Res.* **67,** 3036–3042
85. Wu, J. J., Zhang, X. D., Gillespie, S., and Hersey, P. (2005) *FEBS Lett.* **579,** 1940–1944
86. Bennett, M., Macdonald, K., Chan, S. W., Luzio, J. P., Simari, R., and Weissberg, P. (1998) *Science* **282,** 290–293
87. Robertson, M. J., Kahl, B. S., Vose, J. M., de Vos, S., Laughlin, M., Flynn, P. J., Rowland, K., Cruz, J. C., Goldberg, S. L., Musib, L., Darstein, C., Enas, N., Kutok, J. L., Aster, J. C., Neuberg, D., Savage, K. J., LaCasce, A., Thornton, D., Slapak, C. A., and Shipp, M. A. (2007) *J. Clin. Oncol.* **25,** 1741–1746
88. Wen, J., Ramadevi, N., Nguyen, D., Perkins, C., Worthington, E., and Bhalla, K. (2000) *Blood* **96,** 3900–3906
89. Gibson, S. B., Oyer, R., Spalding, A. C., Anderson, S. M., and Johnson, G. L. (2000) *Mol. Cell. Biol.* **20,** 205–212
90. Johnson, T. R., Stone, K., Nikrad, M., Yeh, T., Zong, W. X., Thompson, C. B., Nesterov, A., and Kraft, A. S. (2003) *Oncogene* **22,** 4953–4963
91. He, Q., Huang, Y., and Sheikh, M. S. (2004) *Oncogene* **23,** 2554–2558
92. Yoshida, T., Shiraishi, T., Nakata, S., Horinaka, M., Wakada, M., Mizutani, Y., Miki, T., and Sakai, T. (2005) *Cancer Res.* **65,** 5662–5667
93. Kim, K., Fisher, M. J., Xu, S. Q., and el-Deiry, W. S. (2000) *Clin. Cancer Res.* **6,** 335–346
94. Mesner, P. W., Jr., Budihardjo, I. I., and Kaufmann, S. H. (1997) *Adv. Pharmacol.* **41,** 461–499
95. Caserta, T. M., Smith, A. N., Gultice, A. D., Reedy, M. A., and Brown, T. L. (2003) *Apoptosis* **8,** 345–352